GENERAL INSTABILITY OF CYLINDRICAL SHELLS

by

S.Y. Lu

and

William A. Nash

Final Report
for
National Aeronautics and Space Administration
Washington, D.C.

Research Grant No. NsG-16-59

Department of Engineering Science and Mechanics
Engineering and Industrial Experiment Station
College of Engineering
University of Florida
Gainesville, Florida

April, 1965

GENERAL INSTABILITY OF CYLINDRICAL SHELLS

by

S. Y. Lu

and

William A. Nash

Final Report
for
National Aeronautics and Space Administration
Washington, D. C.

Research Grant No. NsG-16-59

Department of Engineering Science and Mechanics
Engineering and Industrial Experiment Station
College of Engineering
University of Florida
Gainesville, Florida

April, 1965

given in Parts I and II. The nomenclature, figures, and references are listed in the parts in which they are used, so that each part can be read without referring to the other parts of this report. However, the same notation is used throughout.

SUMMARY

The present investigation is concerned with the general instability of elastic cylindrical shells. Nonlinear finite-deflection theory is employed throughout in the analysis. The nonlinearity is due to the inclusion of second-order terms in the strain-displacement relations. The linear theory is the limiting case when the deflection is very small.

The investigation is divided into five parts. The first of these is concerned with the postbuckling behavior of thin pressurized cylinders subject to bending or compression. In the second part the effects of imperfections of pressurized cylinders under compression are considered. The third part is concerned with the stability of ring-stiffened cylindrical shells under internal pressure and axial compression or bending. The fourth part deals with the problem of buckling of a ring-stiffened shell subjected to external pressure; and, in the fifth, the effect of surface shear on buckling of cylindrical shells is observed upon examining the compatibility equation and equilibrium equation.

Solutions for Parts I, II, and III were obtained by using the Galerkin method. The method of minimum potential energy was employed in Part IV. Numerical solutions are

PART I

ELASTIC INSTABILITY OF PRESSURIZED CYLINDRICAL SHELLS UNDER COMPRESSION OR BENDING

Introduction

The postbuckling behavior of cylindrical shells subject to axial compression has been studied by several investigators. Donnell [I-1] first derived the governing finite-deflection equations; later, in 1941, these equations were used by von Karman and Tsien [I-2] to obtain an approximate solution to the problem of buckling of an axially compressed cylinder into a diamond-shaped buckle pattern. Further investigation was made by Kempner [I-3] who used an additional parameter in the buckling deflection function proposed in [I-2]. Several variations of these analyses have been proposed by other investigators.

The increase in stability of internally pressurized cylindrical shells subject to axisymmetric loading was studied by Lo, Crate, and Schwartz [I-4]. They used large-deflection theory and found that the critical stress increases from a value of 0.37 Et/R at zero pressure to 0.606 Et/R (i.e., the value given by classical small-deflection theory) as the pressure increases to 0.2 Et^2/R^2. The effect of internal pressurization on stability of axially compressed cylinders was studied by Thielemann [I-5]. In addition to presenting a finite-deflection theory, he also conducted tests on aluminum shells. All the aforementioned analytical solutions were obtained on the basis of the energy criterion.

Seide [I-6] has presented a linear small-deflection analysis of the buckling of cylindrical shells subject to pure bending. This study indicated that, contrary to the commonly accepted value, the maximum critical bending stress is for all practical purposes equal to the critical stress found for axial compression. This result, based upon small-deflection theory, does not offer any explanation of the experimental differences known to exist for these two situations. For example, experimental evidence due to Suer, Harris, Skene, and Benjamin [I-7] indicates buckling loads in bending to be from 25 to 60 per cent greater than in compression, the exact value depending upon the ratio R/t.

This part of the report is a study of the elastic post-buckling behavior of thin pressurized cylinders subject to bending loads. Throughout this analysis, the Galerkin method is employed. For comparison with certain existing results obtained by using the energy method, a solution for shells subject to axisymmetric compression is reached first. For this case, when the pressure parameter pR^2/Et^2 approaches unity, it is found that the solution is the same as the classical small-deflection solution.

The relation of the critical stress to internal pressure has been found. For this purpose it is convenient to introduce as a parameter the ratio between the increment of critical stress and the critical stress at zero pressure. This parameter will be essentially independent of the imperfections in the shell when the imperfections do not vary significantly due to changes in pressure. Finally, experimental data due to Suer, Harris, Skene, and Benjamin [I-7] are compared with the results of the present analysis.

Nomenclature

D	Flexural rigidity $Et^3/12(1-\nu^2)$
E	Young's modulus
F	Airy stress function
R	Radius of middle surface of shell
m, n	Number of waves in axial and circumferential directions, respectively
p	Internal pressure
t	Wall thickness of shell
w	Radial deflection
x, s	Co-ordinates of a point in the middle surface of the shell, measured in the longitudinal and circumferential directions respectively
α	R/tm^2
η	$b_3/t\alpha$
μ	n^2/m^2
ν	Poisson's ratio, $\nu = 0.3$ in present study

ϕ, ϕ_b	Dimensionless stress parameters
σ, σ_b, σ_c	Axial compressive stresses
∇^2	Laplace operator
∇^4	$(\nabla^2)^2$

Subscripts:

b	Bending
cr	Critical condition
o	No pressure

Basic Equations and Deflection Function

For an initially perfect thin cylindrical shell the compatibility and equilibrium equations can be expressed, respectively, as

$$\nabla^4 F - E\left[\left(\frac{\partial^2 w}{\partial x \partial s}\right)^2 - \frac{\partial^2 w}{\partial x^2}\frac{\partial^2 w}{\partial s^2} - \frac{1}{R}\frac{\partial^2 w}{\partial x^2}\right] = 0 \tag{I-1}$$

$$D\nabla^4 w - \frac{t}{R}\frac{\partial^2 F}{\partial x^2} - t\left[\frac{\partial^2 F}{\partial s^2}\frac{\partial^2 w}{\partial x^2} - 2\frac{\partial^2 F}{\partial x \partial s}\frac{\partial^2 w}{\partial x \partial s} + \frac{\partial^2 F}{\partial x^2}\frac{\partial^2 w}{\partial s^2}\right] + P = 0 \tag{I-2}$$

In the above equations, F is the Airy stress function of the membrane stresses, w is the radial deflection, t the shell thickness, R the radius of the middle surface, and p is internal pressure (taken to be positive).

An approximate form of the deflection pattern is assumed:

$$w = b_1 + \cos^{\gamma}\left(\frac{ks}{2R}\right)\left[b_2 \cos\frac{mx}{R} \cos\frac{ns}{R} + b_3 \cos\frac{2mx}{R} + b_3 \cos\frac{2ns}{R}\right] \qquad \text{(I-3)}$$

where $k = \begin{cases} 0 & \text{for a shell subject to axial compression} \\ 1 & \text{for a shell subject to eccentric compression or pure bending} \end{cases}$

$\gamma =$ even integer

and m and n represent the number of waves in the axial and circumferential directions respectively, the number of waves in the axial direction being within a length equal to the circumference of the cylinder. Throughout the present study $\gamma = 2$. For more localized buckling, a larger value of γ could be used. When k = 0, (I-3) is the same as that used in [I-2] . In (I-3) , b_1 is not an independent parameter but is used to satisfy the condition of periodicity of circumferential displacement [I-3] . Corresponding to (I-3) , an expression for the stress function F is proposed

$$F = -\frac{\sigma_c}{2} s^2 + \sigma_b R^2 \cos\frac{s}{R} + \frac{1}{2}\frac{pR}{t} x^2 + a_{11} \cos\frac{mx}{R} \cos\frac{ns}{R}$$

$$+ a_{22} \cos\frac{2mx}{R} \cos\frac{2ns}{R} + a_{20} \cos\frac{2mx}{R} + a_{02} \cos\frac{2ns}{R} \qquad \text{(I-4)}$$

The stresses σ_c and σ_b are due to axial compression and bending, respectively, and are positive for compression. For shells subject to axisymmetric compression only, $\sigma_b = 0$ and σ_c is replaced by σ to avoid any possible confusion in notation.

Method of Solution

When w and F in (I-3) and (I-4) are substituted in (I-1) and (I-2), the equalities generally will not hold. They can, however, be expressed instead as

$$\nabla^4 F - E\left[\left(\frac{\partial^2 w}{\partial x \partial s}\right)^2 - \frac{\partial^2 w}{\partial x^2}\frac{\partial^2 w}{\partial s^2} - \frac{1}{R}\frac{\partial^2 w}{\partial x^2}\right] = Q_1 \qquad \text{(I-5)}$$

and

$$D\nabla^4 w - \frac{t}{R}\frac{\partial^2 F}{\partial x^2} - t\left[\frac{\partial^2 F}{\partial s^2}\frac{\partial^2 w}{\partial x^2} - 2\frac{\partial^2 F}{\partial x \partial s}\frac{\partial^2 w}{\partial x \partial s} + \frac{\partial^2 F}{\partial x^2}\frac{\partial^2 w}{\partial s^2}\right]$$

$$+ P = Q_2 \tag{I-6}$$

An approximate solution is obtained by minimizing Q_1 and Q_2 on the right-hand sides of the above equations; this is done by the Galerkin method.

The Galerkin method establishes the following set of equations:

$$\left.\begin{aligned}
&\int_0^L\int_0^{2\pi R} Q_1 \cos\frac{mx}{R}\cos\frac{ns}{R}\,ds\,dx = 0\\
&\int_0^L\int_0^{2\pi R} Q_1 \cos\frac{2mx}{R}\cos\frac{2ns}{R}\,ds\,dx = 0\\
&\int_0^L\int_0^{2\pi R} Q_1 \cos\frac{2mx}{R}\,ds\,dx = 0\\
&\int_0^L\int_0^{2\pi R} Q_1 \cos\frac{2ns}{R}\,ds\,dx = 0
\end{aligned}\right\} \tag{I-7}$$

$$\left.\begin{aligned} &\int_0^L\int_0^{2\pi R} Q_2 \cos\frac{mx}{R}\cos\frac{ns}{R}\cos^2\left(\frac{ks}{2R}\right) ds\,dx = 0 \\ &\int_0^L\int_0^{2\pi R} Q_2 \left(\cos\frac{2mx}{R} + \cos\frac{2ns}{R}\right)\cos^2\left(\frac{ks}{2R}\right) ds\,dx = 0 \end{aligned}\right\} \qquad \text{(I-8)}$$

Again, k = 0 when the shell is subject to axial compression only. In the following sections, solutions are obtained for axial compression and bending separately, although the approaches are the same.

Axisymmetric Compression

In this section, the parameter k in (I-3) and (I-8) and also σ_b in (I-4) are zero. Also, σ_c in (I-4) is replaced by σ. The coefficients a_{20}, a_{02}, a_{11}, and a_{22} appearing in (I-4) can be expressed in terms of b_2 and b_3 through the four integrals of (I-7). The relations are found to be

$$\frac{a_{20}}{Et^2} = \frac{1}{16}\left[-\frac{\mu}{2}\left(\frac{b_2}{t}\right)^2 + 4\eta\alpha^2\right], \quad \frac{a_{02}}{Et^2} = -\frac{1}{32\mu}\left(\frac{b_2}{t}\right)^2$$

$$\frac{a_{11}}{Et^2} = \frac{\alpha}{(1+\mu)^2}(1-4\mu\eta)\frac{b_2}{t}, \quad \frac{a_{22}}{Et^2} = -\frac{\mu\eta^2\alpha^2}{(1+\mu)^2} \qquad \text{(I-9)}$$

In the above expressions, the dimensionless parameters are defined so that

$$\mu = \frac{n^2}{m^2} \tag{I-10}$$

$$\alpha = \frac{1}{m^2} \cdot \frac{R}{t} \tag{I-11}$$

$$\eta = \frac{b_3}{t\alpha} \tag{I-12}$$

The ratio n/m evidently represents the wave-length ratio in axial/circumferential directions.

The integration of (I-8) together with the relations given in (I-9) leads to the following two equations:

$$\alpha\phi = \frac{(1+\mu)^2}{12(1-\nu^2)} + \left\{ \frac{1}{(1+\mu)^2} - \left[\frac{8}{(1+\mu)^2} + \frac{1}{2} \right] \mu\eta \right.$$

$$\left. + \frac{16}{(1+\mu)^2} \mu^2\eta^2 \right\} \alpha^2 + \frac{1+\mu^2}{16} \left(\frac{b_2}{t} \right)^2 \tag{I-13}$$

$$\alpha\phi = \frac{1+\mu^2}{3(1-\nu^2)} + \left[\frac{1}{4} + \frac{4\mu^2}{(1+\mu)^2}\eta^2\right]\alpha^2 + \left\{\frac{2\mu^2}{(1+\mu)^2}\right.$$

$$\left. - \left[\frac{1}{2}\frac{1}{(1+\mu)^2} + \frac{1}{32}\right]\frac{\mu}{\eta}\right\}\left(\frac{b_2}{t}\right)^2 \qquad \text{(I-14)}$$

The function ϕ on the left-hand sides of the above equations is a nondimensional stress parameter defined by the relation

$$\phi = \frac{\sigma R}{Et} - \mu\frac{pR^2}{Et^2} \qquad \text{(I-15)}$$

For brevity, (I-13) and (I-14) may be rewritten as:

$$\alpha\phi = A_1 + (A_2 + A_3\eta + A_4\eta^2)\alpha^2 + A_5\left(\frac{b_2}{t}\right)^2 \qquad \text{(I-13a)}$$

$$\alpha\phi = B_1 + (B_2 + B_4\eta^2)\alpha^2 + \left(B_5 + \frac{B_6}{\eta}\right)\left(\frac{b_2}{t}\right)^2 \qquad \text{(I-14a)}$$

where

$$\left.\begin{aligned}
A_1 &= \frac{(1+\mu)^2}{12(1-\nu^2)} , & A_2 &= \frac{1}{(1+\mu)^2} \\
A_3 &= -\left[\frac{8}{(1+\mu)^2} + \frac{1}{2}\right]\mu , & A_4 &= \frac{16\mu^2}{(1+\mu)^2} \\
A_5 &= \frac{1+\mu^2}{16} , & B_1 &= \frac{1+\mu^2}{3(1-\nu^2)} \\
B_2 &= \frac{1}{4} , & B_4 &= \frac{4\mu^2}{(1+\mu)^2} \\
B_5 &= \frac{2\mu^2}{(1+\mu)^2} , & B_6 &= -\left[\frac{1}{2(1+\mu)^2} + \frac{1}{32}\right]\mu
\end{aligned}\right\} \tag{I-16}$$

The parameter (b_2/t) is eliminated between (I-13a) and (I-14a) and the stress parameter ϕ is expressed as

$$\phi = \frac{C_1 A_1}{\alpha} + C_2 A_2 \alpha \tag{I-17}$$

In the above equation,

$$C_1 = \frac{\frac{A_5}{A_1} B_1 - B_5 - \frac{B_6}{\eta}}{A_5 - B_5 - \frac{B_6}{\eta}} \tag{I-18}$$

$$C_2 = \frac{\left(\frac{A_5}{A_2} B_2 - \frac{A_3}{A_2} B_6 - B_5\right) - \frac{B_6}{\eta} - \left(\frac{A_3}{A_2} B_5 + \frac{A_4}{A_2} B_6\right)\eta + \left(\frac{A_5}{A_2} B_4 - \frac{A_4}{A_2} B_5\right)\eta^2}{A_5 - B_5 - \frac{B_6}{\eta}} \tag{I-19}$$

As can be seen from (I-15) to (I-19) the dimensionless variable $\sigma R/Et$ is a function of α, η, and μ. The buckling stress is thus obtained through minimization with respect to the parameters α, η, and μ. Differentiation of ϕ with respect to α is carried out first to obtain

$$\frac{\partial \phi}{\partial \alpha} = \frac{\partial \sigma}{\partial \alpha} = 0 \tag{I-20}$$

for p = constant. Thus from (I-17) :

$$\alpha = \sqrt{\frac{C_1 A_1}{C_2 A_2}} \tag{I-21}$$

and finally from (I-17) with α given by (I-21)

$$\phi_\alpha = 2\sqrt{A_1 A_2}\sqrt{C_1 C_2} \tag{I-22}$$

The notation ϕ_α thus denotes the value of ϕ minimized with respect to α . The expressions for C_1 and C_2 are found from (I-18) , (I-19) , and (I-16) . From (I-16)

$$\phi_\alpha = \sqrt{C_1 C_2}\sqrt{\frac{1}{3(1-\nu^2)}} \tag{I-22a}$$

It should be noted that $\sqrt{1/3(1-\nu^2)}$ is the classical coefficient from small-deflection theory for an unpressurized shell. When $\nu = 0.3$, $\sqrt{1/3(1-\nu^2)} = 0.606$. The minimization of ϕ with respect to η and μ is most easily obtained by numerical, or, rather, by graphic means. This is done by plotting ϕ_α in (I-22a) against η for each given value of μ . The minimum ϕ_α found from each of these curves is called $\phi_{\alpha,\eta}$, which should be equivalent to the value found from the relation $\partial\phi_\alpha/\partial\eta = 0$. Table I-1 gives some of the numerical relations obtained in the course of this procedure.

TABLE I-1

$\mu = 0$	0.2	0.25	0.5	1.0	1.15
$\eta =$	0.59	0.53	0.325	0.18	0.11
$\phi_{\alpha,\eta} = 0.605$	0.44	0.406	0.29	0.19	0.161

Let us introduce the following dimensionless parameters

$$\bar{\sigma} = \frac{\sigma R}{Et} \tag{I-23}$$

and

$$\bar{p} = \frac{pR^2}{Et^2} \tag{I-24}$$

Then (I-15) may be rewritten as

$$\bar{\sigma}_{\alpha,\eta} = \phi_{\alpha,\eta} + \mu \bar{p} \qquad \text{(I-25)}$$

where $\bar{\sigma}_{\alpha,\eta}$ represents the minimized value of $\bar{\sigma}$ with respect to α and η. To find the dimensionless critical stress $\bar{\sigma}_{cr}$ at a given value of dimensionless pressure $\bar{p}$, several different values of μ are tried in (I-25) together with corresponding values of $\phi_{\alpha,\eta}$ from Table I-1 until the right-hand side of (I-25) is minimized. The value of μ, at which $\bar{\sigma}_{\alpha,\eta}$ is minimum and equals $\bar{\sigma}_{cr}$, is called μ_{cr}. Some values of $\bar{\sigma}_{cr}$ and μ_{cr} for various values of $\bar{p}$ are given in Table I-2.

TABLE I-2

$\bar{p}$ = 0	0.01	0.05	0.1	0.2	0.4	0.6	0.8
μ_{cr} = 1.15	1.10	1.08	1.04	0.76	0.45	0.24	0.08
$\bar{\sigma}_{cr}$ = 0.161	0.176	0.227	0.283	0.37	0.481	0.56	0.6

It can be seen that μ_{cr} decreases with increasing $\bar{p}$. This indicates that the buckling wave becomes longer in the circumferential direction when the pressure increases.

The relation between $\bar{\sigma}_{cr}$ and $\bar{p}$ is shown in Fig. I-1 as

Curve II. The results from [I-4] and [I-5] and the test data from [I-8] and [I-9] are plotted in this figure also. The broken curve shown there represents the curve best fitting the data in [I-5], [I-8], and [I-9]. The predictions of the present theory are shown as Curve II in Fig. II-2 so as to afford a comparison with experimental data given in [I-7].

In Fig. I-1, the broken curve indicates that $\bar{\sigma}_{cr}$ is only about 0.09 at $\bar{p} = 0$, and $\bar{\sigma}_{cr}$ increases from 0.09 to approximately 0.35, then levels off at higher values of $\bar{p}$. However, $\bar{\sigma}_{cr}$ is expected to reach the classical value of 0.606 when the value of $\bar{p}$ is relatively high. One of the most probable causes of the lower result indicated by the broken curve corresponding to test data lies in initial imperfections which in general increase with increasing R/t. If the imperfection factor does not vary significantly due to the change of $\bar{p}$, then the ratio of $\bar{\sigma}_{cr}$ at two different pressures will be nearly independent of the effect of imperfections. Let $\bar{\sigma}_{cr,o}$ represent $\bar{\sigma}_{cr}$ at $\bar{p} = 0$, and

$$\Delta \bar{\sigma}_{cr} = \bar{\sigma}_{cr} - \bar{\sigma}_{cr,o}$$

The ratio, $\Delta\bar{\sigma}_{cr}/\bar{\sigma}_{cr,o}$, is plotted against $\bar{p}$ in Fig. I-3. As shown in this figure, the predictions of the present theory are in reasonably good agreement with experimental evidence, which is re-plotted from the broken curve of Fig. I-1. One advantage of introducing the ratio $\Delta\bar{\sigma}_{cr}/\bar{\sigma}_{cr,o}$ is that the relation in Fig. I-3 can be used having test data at only one pressure to predict the critical stress in the same imperfect shell at any other pressure. For instance, a test is made at $\bar{p} = 0.4$, for which value $\bar{\sigma}_{cr}$ is found experimentally to be 0.29. From Fig. I-3, the present analysis gives $\Delta\bar{\sigma}_{cr}/\bar{\sigma}_{cr,o} = 2.02$. Therefore, it can be predicted that $\bar{\sigma}_{cr} = 0.096$, 0.221, and 0.356 at $\bar{p} = 0$, 0.2, and 0.8, respectively, while the mean test data from Fig. I-1 show that $\bar{\sigma}_{cr} = 0.09$, 0.25, and 0.34 at $\bar{p} = 0$, 0.2, and 0.8, respectively.

Eccentric Compression, Pure Bending

When a cylindrical shell is subject either to pure bending or eccentrically applied compression, k in (I-3) and (I-8) is unity. The solution in this case is analogous to the solution of the previous section. The coefficients of the Airy stress function F are found to be

$$\left.\begin{aligned}
\frac{a_{20}}{Et^2} &= \frac{1}{16}\left[2\eta\alpha^2 - \left(\frac{3}{16}\mu + \frac{1}{16m^2}\right)\left(\frac{b_2}{t}\right)^2\right] \\
\frac{a_{02}}{Et^2} &= -\frac{3}{256\mu}\left(\frac{b_2}{t}\right)^2 \\
\frac{a_{11}}{Et^2} &= \frac{\alpha\left[1-\left(3\mu+\frac{1}{4m^2}\right)\eta\right]\left(\frac{b_2}{t}\right)}{2(1+\mu)^2} \\
\frac{a_{22}}{Et^2} &= -\frac{\left(6\mu+\frac{1}{2m^2}\right)\eta^2\alpha^2 + \frac{1}{16m^2}\left(\frac{b_2}{t}\right)^2}{16(1+\mu)^2}
\end{aligned}\right\} \tag{I-26}$$

where μ, α, and η are given by (I-10) , (I-11) , and (I-12) , respectively.

From (I-8) and (I-26)

$$\alpha\phi_1 = \frac{1}{(1-\nu^2)}\left[\frac{(1+\mu)^2}{8} + \frac{1}{12m^2}\left(1+3\mu+\frac{1}{2m^2}\right)\right] + \left\{\frac{1}{(1+\mu)^2}\right.$$

$$\left. - \left[\frac{6\mu+\frac{1}{2m^2}}{(1+\mu)^2} + \frac{3\mu+\frac{1}{m^2}}{8}\right]\eta + \left[\frac{576\mu^2+108\frac{\mu}{m^2}+\frac{5}{m^4}}{64(1+\mu)^2}\right]\eta^2\right\}\alpha^2$$

$$+\left[\frac{9+9\mu^2+\frac{6\mu}{m^2}+\frac{1}{m^4}}{256} + \frac{1}{m^4}\cdot\frac{1}{512(1+\mu)^2}\right]\left(\frac{b_2}{t}\right)^2 \tag{I-27}$$

$$\alpha \phi_2 = \frac{1}{2(1-\nu^2)}\left[(1+\mu^2) + \frac{1}{6m^2}\left(1+3\mu+\frac{1}{4m^2}\right)\right]$$

$$+\left[\frac{1}{4} + \left\{\frac{144\mu^2 + \frac{24\mu}{m^2} + \frac{1}{m^4}}{64(1+\mu)^2}\right\}\eta^2\right]\alpha^2$$

$$+\left\{\frac{576\mu^2 + 108\frac{\mu}{m^2} + \frac{5}{m^4}}{512(1+\mu)^2} - \left[\frac{12\mu + \frac{1}{m^2}}{32(1+\mu)^2} + \frac{3\mu + \frac{1}{m^2}}{128}\right]\frac{1}{\eta}\right\}\left(\frac{b_2}{t}\right)^2 \tag{I-28}$$

The stress parameters ϕ_1 and ϕ_2 are defined by the relations

$$\phi_1 = \frac{\sigma_b R}{Et} + \frac{3}{2}\cdot\frac{\sigma_c R}{Et} - \frac{1}{2}\left(3\mu + \frac{1}{m^2}\right)\frac{pR^2}{Et^2}$$

$$\phi_2 = \frac{\sigma_b R}{Et} + \frac{3}{2}\cdot\frac{\sigma_c R}{Et} - \frac{1}{2}\left(3\mu + \frac{1}{2m^2}\right)\frac{pR^2}{Et^2} \tag{I-29}$$

The experiments of Suer, Harris, Skene, and Benjamin [I-7] indicate that shells subject to compression or bending will buckle into a multiple wave pattern in the longitudinal direction. Numerical results from the present analysis also indicate that m has a magnitude greater than 10 when R/t is greater than 500. These calculations are too lengthy to present, but for example: At $\bar{p} = 0.48$ and $R/t = 1{,}000$, it was found that $1/m^2 = 0.00204$, which is much less than unity. The value of α is usually in the neighborhood of unity; hence, from (I-11) m^2 varies approximately as R/t. In the present analysis we are concerned only with extremely thin shells; hence this ratio is large. Therefore, for practical purposes $1/m^2$ and $1/m^4$ are negligible compared to unity. Thus,

$$\phi_1 = \phi_2 = \phi_b = \frac{\sigma_b R}{Et} + \frac{3}{2}\frac{\sigma_c R}{Et} - \frac{3}{2}\mu\frac{pR^2}{Et^2} \qquad \text{(I-30)}$$

$$\alpha\phi_b = \frac{1}{(1-\nu^2)}\cdot\frac{(1+\mu)^2}{8} + \left\{\frac{1}{(1+\mu)^2} - \mu\left[\frac{6}{(1+\mu)^2} + \frac{3}{8}\right]\eta + \frac{9\mu^2}{(1+\mu)^2}\eta^2\right\}\alpha^2 + \frac{9(1+\mu)^2}{256}\left(\frac{b_2}{t}\right)^2 \qquad \text{(I-31)}$$

and

$$\alpha\,\phi_b = \frac{1+\mu^2}{2(1-\nu^2)} + \left[\frac{1}{4} + \frac{9\mu^2}{4(1+\mu)^2}\eta^2\right]\alpha^2$$

$$+\left\{\frac{9}{8}\cdot\frac{\mu^2}{(1+\mu)^2} - \left[\frac{1}{8(1+\mu)^2} + \frac{1}{128}\right]\frac{3\mu}{\eta}\right\}\left(\frac{b_2}{t}\right)^2 \qquad \text{(I-32)}$$

For brevity, (I-31) and (I-32) may be rewritten as:

$$\alpha\;\phi_b = \bar{A}_1 + (\bar{A}_2 + \bar{A}_3\eta + \bar{A}_4\eta^2)\alpha^2 + \bar{A}_5\left(\frac{b_2}{t}\right)^2 \qquad \text{(I-31a)}$$

and

$$\alpha\;\phi_b = \bar{B}_1 + (\bar{B}_2 + \bar{B}_4\eta^2)\alpha^2 + \left(\bar{B}_5 + \frac{\bar{B}_6}{\eta}\right)\left(\frac{b_2}{t}\right)^2 \qquad \text{(I-32a)}$$

where

$$\bar{A}_1 = \frac{(1+\mu)^2}{8(1-\nu^2)} \quad , \quad \bar{A}_2 = \frac{1}{(1+\mu)^2}$$

$$\bar{A}_3 = -\left[\frac{6}{(1+\mu)^2} + \frac{3}{8}\right] \quad , \quad \bar{A}_4 = \frac{9\mu^2}{(1+\mu)^2}$$

$$\bar{A}_5 = \frac{9(1+\mu^2)}{256} \quad , \quad \bar{B}_1 = \frac{1+\mu^2}{2(1-\nu^2)}$$

$$\bar{B}_2 = \frac{1}{4} \quad , \quad \bar{B}_4 = \frac{9\mu^2}{4(1+\mu)^2}$$

$$\bar{B}_5 = \frac{9\mu^2}{8(1+\mu)^2} \quad , \quad \bar{B}_6 = -\left[\frac{3}{8(1+\mu)^2} + \frac{3}{128}\right]\mu \qquad \text{(I-33)}$$

Further,

$$\bar{C}_1 = \frac{\frac{\bar{A}_5}{\bar{A}_1}\bar{B}_1 - \bar{B}_5 - \frac{\bar{B}_6}{\eta}}{\bar{A}_5 - \bar{B}_5 - \frac{\bar{B}_6}{\eta}}$$

$$\bar{C}_2 = \frac{\frac{\bar{A}_5}{\bar{A}_2}\bar{B}_2 - \bar{B}_5 - \frac{\bar{A}_3}{\bar{A}_2}\bar{B}_6 - \frac{\bar{B}_6}{\eta} - \left(\frac{\bar{A}_3}{\bar{A}_2}\bar{B}_5 + \frac{\bar{A}_4}{\bar{A}_2}\bar{B}_6\right)\eta + \left(\frac{\bar{A}_5}{\bar{A}_2}\bar{B}_4 - \frac{\bar{A}_4}{\bar{A}_2}\bar{B}_5\right)\eta^2}{\bar{A}_5 - \bar{B}_5 - \frac{\bar{B}_6}{\eta}} \qquad \text{(I-34)}$$

The simultaneous solution of (I-31a) and (I-32a) leads to

$$\phi_b = \frac{\bar{C}_1 \bar{A}_1}{\alpha} + \bar{C}_2 \bar{A}_2 \alpha \tag{I-35}$$

From the relation $\partial \phi_b / \partial \alpha = 0$ and (I-35) ,

$$\alpha = \sqrt{\frac{\bar{C}_1 \bar{A}_1}{\bar{C}_2 \bar{A}_2}} \tag{I-36}$$

and finally from (I-35) with α given by (I-36)

$$(\phi_b)_\alpha = 2\sqrt{\bar{A}_1 \bar{A}_2}\sqrt{\bar{C}_1 \bar{C}_2} = \sqrt{\bar{C}_1 \bar{C}_2}\sqrt{\frac{1}{2(1-\nu^2)}} \tag{I-37}$$

where $(\phi_b)_\alpha$ is the value of ϕ_b minimized with respect to α. For classical small-deflection theory, $\eta = 0$; hence, $C_1 = C_2 = 1$ and the expression $\sqrt{1/2(1-\nu^2)}$ is the coefficient for this theory. When $\nu = 0.3$, $\sqrt{1/2(1-\nu^2)} = 0.74$.

Analogous to the solution in the case of axisymmetric compression, the minimization of ϕ_b with respect to μ and η is done graphically. First, $(\phi_b)_\alpha$ versus η is plotted for various values of μ. The minimum $(\phi_b)_\alpha$ found from each of these curves is called $(\phi_b)_{\alpha,\eta}$. Table I-3 gives some of the numerical relations obtained in the course of this procedure.

TABLE I-3

μ	= 0	0.25	0.5	1.0	1.15
η	=	0.66	0.46	0.23	0.15
$(\phi_b)_{\alpha,\eta}$	= 0.74	0.52	0.34	0.21	0.195

Let us introduce the following dimensionless parameters

$$\bar{\sigma}_b = \frac{\sigma_b R}{Et} \tag{I-38}$$

and

$$\bar{\sigma}_c = \frac{\sigma_c R}{Et}$$

Thus, from (I-30)

$$\left(\bar{\sigma}_b + \frac{3}{2}\bar{\sigma}_c\right)_{\alpha,\eta} = (\phi_b)_{\alpha,\eta} + \frac{3}{2}\mu\bar{P} \tag{I-39}$$

To find the dimensionless critical stress $\left(\bar{\sigma}_b + \frac{3}{2}\bar{\sigma}_c\right)_{cr}$ at a given value of dimensionless pressure $\bar{p}$, several different values of μ are tried in (I-39), together with corresponding values of $(\phi_b)_{\alpha,\eta}$ from Table I-3 until the right-hand side of (I-39) is minimized.

The value of μ at which $\left(\bar{\sigma}_b + \frac{3}{2}\bar{\sigma}_c\right)_{\alpha,\eta}$ is minimum and equals $\left(\bar{\sigma}_b + \frac{3}{2}\bar{\sigma}_c\right)_{cr}$ is called μ_{cr}. Table I-4 indicates some numerical relations in terms of the pressure.

TABLE I-4

$\bar{p}$	= 0	0.025	0.05	0.1	0.2	0.4	0.6	0.8
μ_{cr}	= 1.14	1.1	1.04	0.86	0.63	0.34	0.14	0.02
$(\bar{\sigma}_b + \frac{3}{2}\bar{\sigma}_c)_{cr}$	= 0.2	0.249	0.294	0.365	0.48	0.64	0.73	0.734
$(\bar{\sigma}_c)^*_{cr}$	= 0.133	0.166	0.196	0.243	0.32	0.426	0.487	0.489

It can be seen that μ_{cr} decreases with increasing $\bar{p}$. In the above table, $(\bar{\sigma}_c)^*_{cr}$ stands for the value of $(\bar{\sigma}_c)_{cr}$ when $\bar{\sigma}_b \rightarrow 0$. The relations between $\left(\bar{\sigma}_b + \frac{3}{2}\bar{\sigma}_c\right)_{cr}$ and $\bar{p}$ as well as $(\bar{\sigma}_c)^*_{cr}$ and $\bar{p}$ are shown in Fig. I-2, in which the data from [I-7] are shown also.

The broken curve shown there bounds test data obtained by Suer, Harris, Skene, and Benjamin [I-7] for axial compression. Bending test data due to these same authors are shown by individual points in Fig. I-2.

Let us introduce the notation

$$\Delta\left(\bar{\sigma}_b + \frac{3}{2}\bar{\sigma}_c\right)_{cr} = \left(\bar{\sigma}_b + \frac{3}{2}\bar{\sigma}_c\right)_{cr} - \left(\bar{\sigma}_b + \frac{3}{2}\bar{\sigma}_c\right)_{cr,o} \qquad \text{(I-40)}$$

where $\left(\bar{\sigma}_b + \frac{3}{2}\bar{\sigma}_c\right)_{cr,o}$ represents the value of $\left(\bar{\sigma}_b + \frac{3}{2}\bar{\sigma}_c\right)_{cr}$ at $\bar{p} = 0$. The ratio $\dfrac{\Delta\left(\bar{\sigma}_b + \frac{3}{2}\bar{\sigma}_c\right)_{cr}}{\left(\bar{\sigma}_b + \frac{3}{2}\bar{\sigma}_c\right)_{cr,o}}$ is plotted against $\bar{p}$ in Fig. I-4. Again, this ratio should predict the critical stress in an imperfect shell from test data at only one pressure.

It has been observed that generally $(\bar{\sigma}_c)^*_{cr}$ is not equal to the value of $\bar{\sigma}_{cr}$ found for axisymmetric compression. The difference is due to the deflection patterns employed. Curves II and III of Fig. I-2 indicate the effect on axial compression of those different patterns and show that even a slight eccentricity in application of load will greatly reduce the buckling stress. $(\bar{\sigma}_c)^*_{cr}$ versus $\bar{p}$ is shown in Fig. I-1 as Curve IV.

Discussion and Conclusions

It can be observed that $\mu = 0$ in the case of ring buckling and, further, $b_3 = \eta = 0$ in the case of small deflections. If either μ or b_3 is zero, the above analysis reduces to a small-deflection solution.

The ratio between stresses, $\left(\bar{\sigma}_b + \frac{3}{2}\bar{\sigma}_c\right)_{cr} \Big/ \bar{\sigma}_{cr}$, is approximately 1.25 and varies only slightly with pressure. Therefore, the ratio $\dfrac{(\bar{\sigma}_c)^*_{cr}}{\bar{\sigma}_{cr}}$ is 0.833. The procedure indicated can be employed when test data at one pressure are available to predict the critical stress in the same imperfect shell at any other pressure. Since more consistent test results can be expected from shells under higher pressures, Figs. I-3 and I-4 are available to predict the buckling stresses when at least one test has been made on some moderately pressurized cylinders. For instance, if the critical pure bending stress, $\left(\bar{\sigma}_b\, R/Et\right)_{cr}$, has been found experimentally as 0.53 at $\bar{p} = 0.4$, then from Fig. I-4 can be found $\left(\sigma_b R/Et\right)_{cr} = 0.163$, and 0.603 at $\bar{p} = 0$, and 0.8, respectively. This evaluation is applied only to shells having the same ratio R/t. The effects due to a change of R/t will be discussed in a later paper.

The predictions of the present theory for pressurized axially compressed cylindrical shells are in substantial agreement with test data for a rather wide range of values of internal pressure. Predictions of the theory for pressurized cylindrical shells in pure bending are in reasonable agreement with experimental evidence for dimensionless internal pressures in excess of 0.1 but are conservative for smaller values of internal pressure.

References (I)

1. Donnell, L. H., "A New Theory for the Buckling of Thin Cylinders Under Axial Compression and Bending," Transactions of the ASME, Vol. 56, No. 11, pp. 795-806, November, 1934.

2. von Kármán, T., and Tsien, H. S., "The Buckling of Thin Cylindrical Shells Under Axial Compression," Journal of the Aeronautical Sciences, Vol. 8, No. 8, pp. 303-312, June, 1941.

3. Kempner, J., "Postbuckling Behavior of Axially Compressed Cylindrical Shells," Journal of the Aeronautical Sciences, Vol. 21, No. 5, pp. 329-335, May, 1954.

4. Lo, H., Crate, H., and Schwartz, E. B., "Buckling of Thin-Walled Cylinder Under Axial Compression and Internal Pressure," NACA TN 2021, January, 1950.

5. Thielemann, W. F., "New Development in the Non-linear Theories of the Buckling of Thin Cylindrical Shells," in Aeronautics and Astronautics, Pergamon Press, New York, pp. 76-121, 1960.

6. Seide, P., and Weingarten, V. I., "On the Buckling of Circular Cylindrical Shells Under Pure Bending," Journal of Applied Mechanics, Vol. 28, No. 1, pp. 112-116, March, 1961.

7. Suer, H. S., Harris, L. A., Skene, W. T., and Benjamin, R. J., "The Bending Stability of Thin-Walled Unstiffened Circular Cylinders Including the Effect of Internal Pressure," Journal of the Aeronautical Sciences, Vol. 25, No. 5, pp. 281-287, 1958.

8. Fung, Y. C., and Sechler, E. E., "Buckling of Thin-Walled Circular Cylinders Under Axial Compression and Internal Pressure," Journal of the Aeronautical Sciences, Vol. 24, No. 5, pp. 351-356, May, 1957.

9. Lofblad, R. P., Jr., "Elastic Stability of Thin-Walled Cylinders and Cones with Internal Pressure Under Axial Compression," MIT Technical Report 25-29, May, 1959.

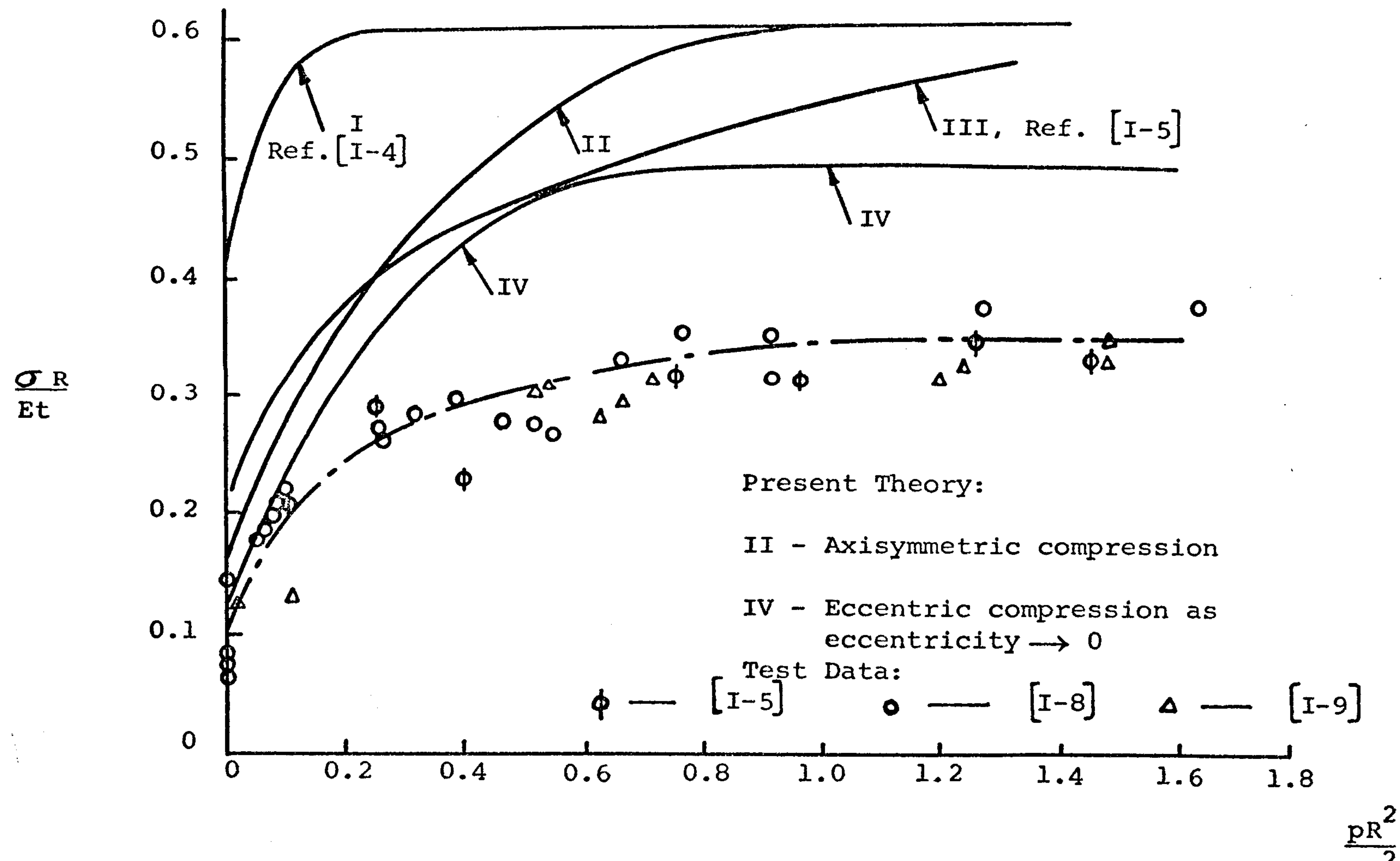

Fig. I-1. Postbuckling Behavior of Axially Compressed Pressurized Cylindrical Shells

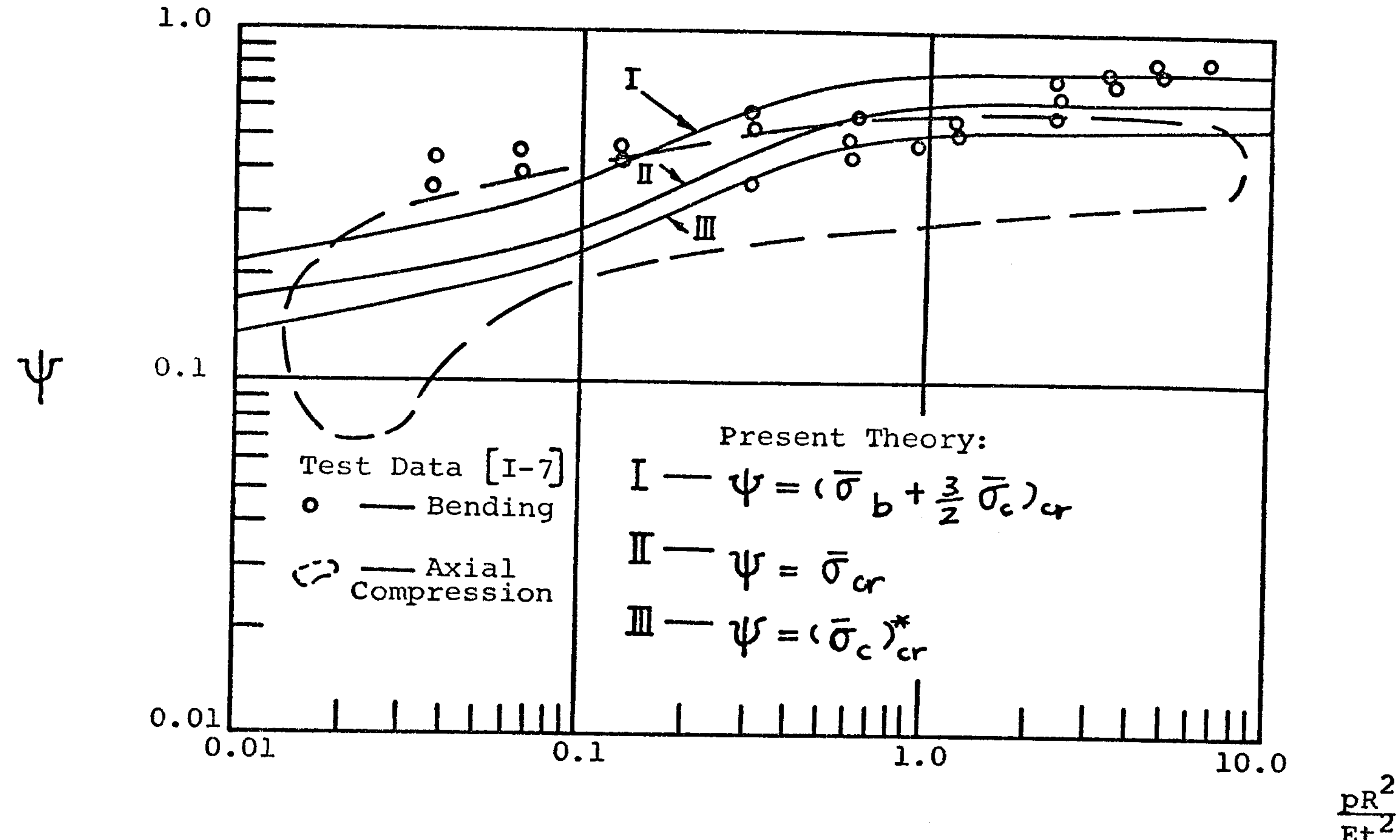

Fig. I-2. Postbuckling Behavior of Pressurized Cylindrical Shells Subject to Bending or Axial Compression

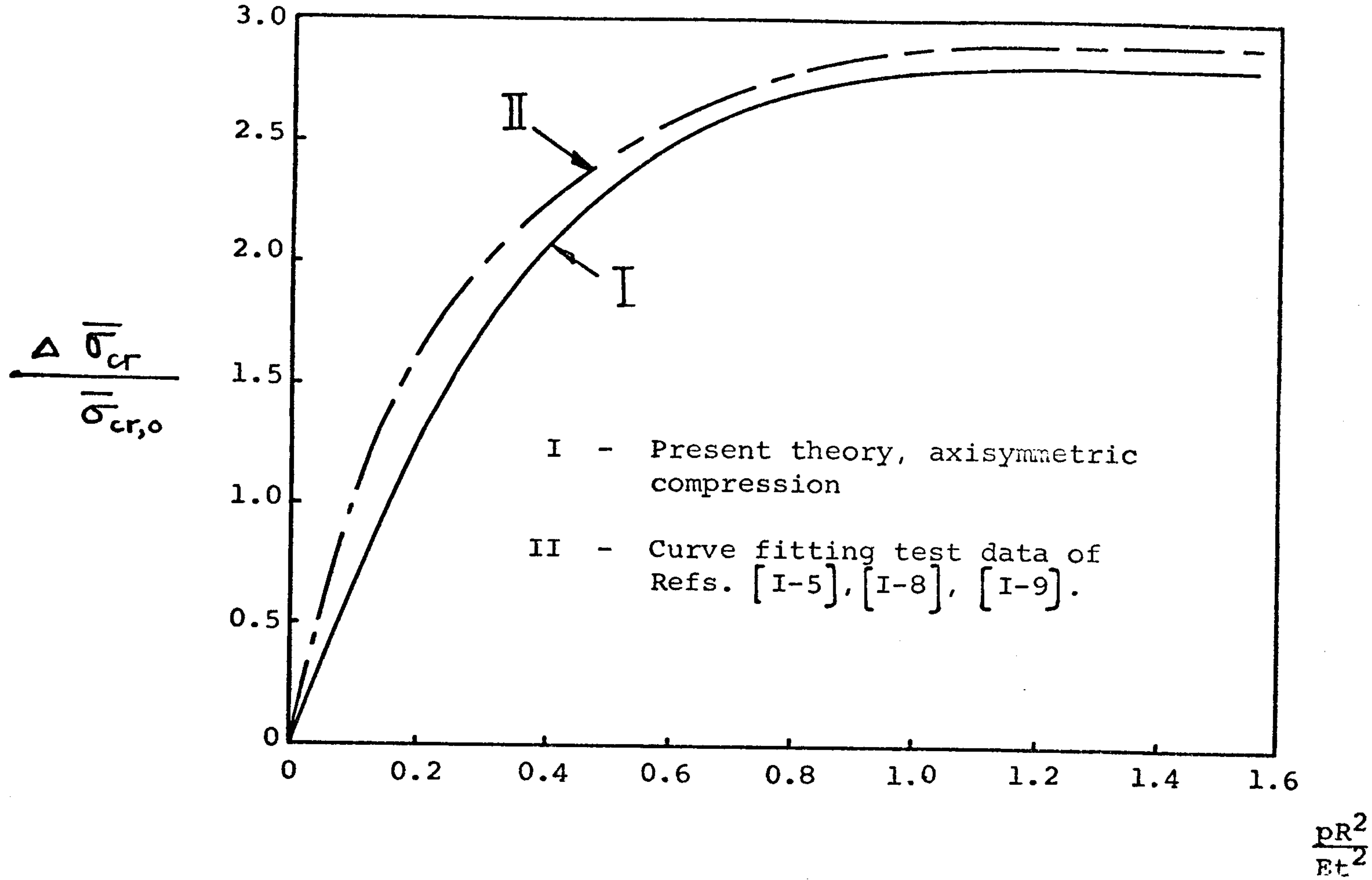

Fig. I-3. Predictions of Present Theory and Test Data for Axially Compressed Pressurized Cylindrical Shells

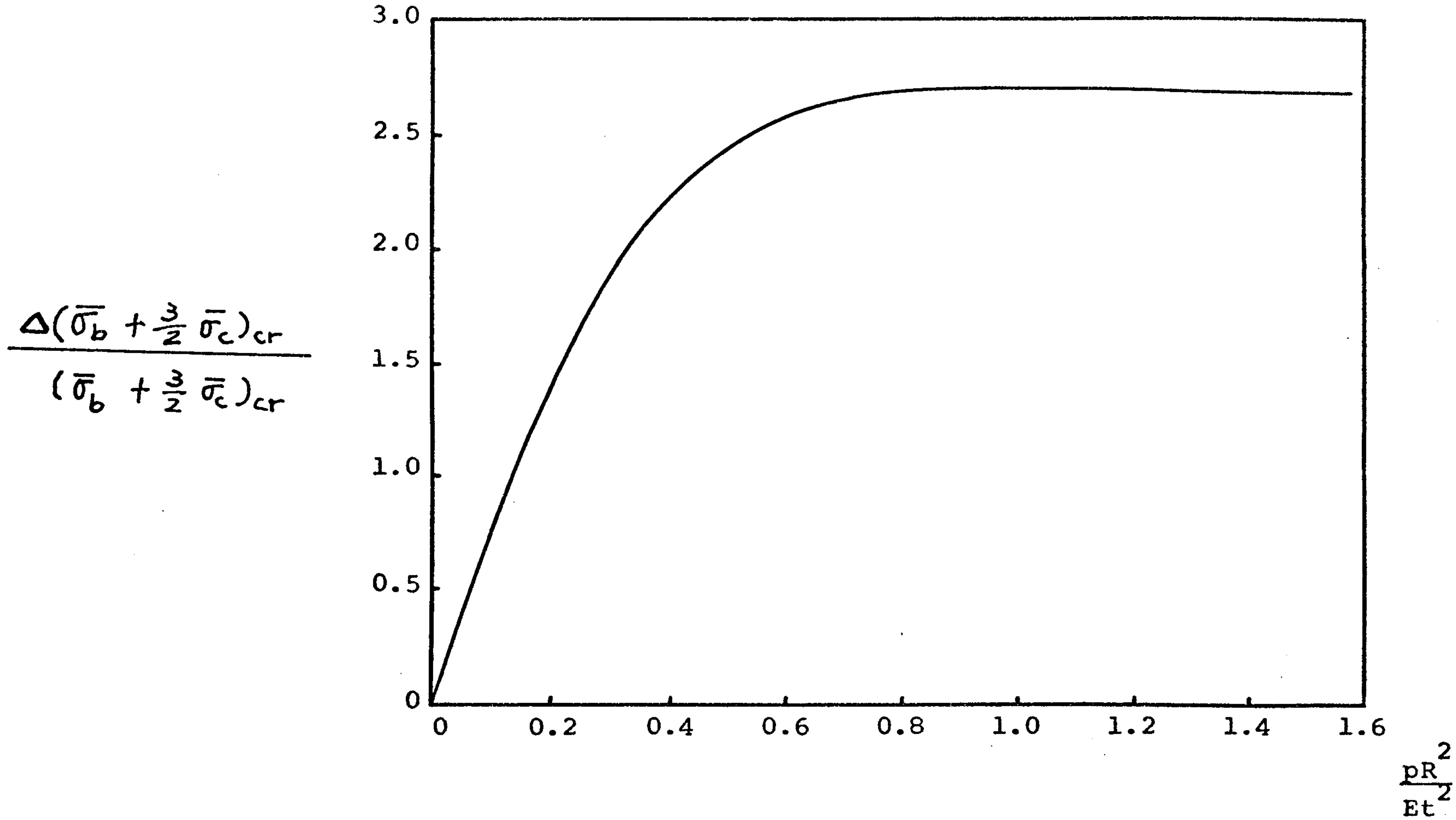

Fig. I-4. Increment of Critical Stress as a Function of Pressure for Cylindrical Shells Subject to Eccentric Compression or Pure Bending

PART II

POSTBUCKLING BEHAVIOR OF PRESSURIZED CYLINDRICAL SHELLS WITH INITIAL DEFLECTION

Introduction

The influence of initial imperfections on buckling strengths was first studied by Donnell in 1934 [II-1]. The solution for cylindrical shells subject to axial compression was later carried out by Donnell and Wan [II-2]. For shells under external pressure, the effects of imperfections and finite deflections have been studied by Nash [II-3], while the case of fixed edges was discussed by Donnell in 1958 [II-4].

The studies made in references [II-1] through [II-4] are based on the assumption that the additional deflection has the same form as the initial deflection, but a different amplitude. In a paper published in 1958, Ivanov [II-5] considered the case of a shell under the action of hydrostatic pressure. His paper is distinctive because the additional deflection assumed wave lengths different from that of the initial deviation.

In the present study, the effects of geometric imperfections on the postbuckling behavior of pressurized cylinders subject to compression are investigated. The total normal deflection is assumed to be different from the initial deviation.

General relations for finding the minimum compression in the postbuckling region are expressed. A linear solution is then deduced from the nonlinear treatment. The smallest value of the minimum stress is found when the additional deflection follows the same form as the initial deflection. This case is treated in the section beginning on page 38. The imperfection factor is introduced in the finite-deflection compatibility and equilibrium equations. A new relation to express the imperfection parameter as an explicit exponential function of both the radius-thickness ratio and the internal pressure is proposed. A method for finding the exponential function is described, and the solution for the critical compression is found in a fairly simple form. The decrease of minimum load with the increasing radius-thickness ratio at different pressure is related.

Nomenclature

C	Index in the exponential function, defined in equation (II-18)
D	Flexural rigidity $Et^3/12(1-\nu^2)$
E	Young's modulus
F	Airy stress function
R	Radius of middle surface of shell
m, n	Number of waves in axial and circumferential directions, respectively

p	Internal pressure
t	Wall thickness of shell
w	Total normal deflection
w_1, w_2	First and second portion of additional deflection, respectively
w_i	Initial deflection
x, s	Co-ordinates of a point in the middle surface of the shell
Γ	$w_i/(w_i + w_1)$, imperfection ratio
α	R/m^2t
η	$(b_3/t)/\alpha$
μ	n^2/m^2
γ	Imperfection coefficient, defined in equation (II-25)
ν	Poisson's ratio, $\nu = 0.3$
∇^4	$\dfrac{\partial^4}{\partial x^4} + 2\dfrac{\partial^4}{\partial x^2 \partial s^2} + \dfrac{\partial^4}{\partial s^4}$
ϕ	Stress parameter, defined in equation (II-21)
σ	Uniform axial compressive stress

Superscript:

o	Perfect shell

Subscript

min	Minimum value

Additional Deflection Different From Initial Deflection

For an imperfect shell, the additional deflection due to load can be considered as being composed of two parts. The first portion assumes the shape of the initial deflection, while the second has a new wave pattern which is different from the initial deviation. The total deformation is, therefore, the sum of the initial deviation and the two parts of the additional deflection. In the following, the non-linear compatibility equation and equilibrium equation are first written and the solution is then obtained by using the Galerkin method to integrate these two equations.

Basic Equation. We let w equal the total radial deflection; w_i, the initial imperfection in the radial direction; and F, the Airy stress function. The finite-deflection compatibility equation has the following form:

$$\nabla^4 F = E\Big[\left(\frac{\partial^2 w}{\partial x \partial s}\right)^2 - \frac{\partial^2 w}{\partial x^2}\frac{\partial^2 w}{\partial s^2} - \frac{1}{R}\frac{\partial^2 w}{\partial x^2} - \left(\frac{\partial^2 w_i}{\partial x \partial s}\right)^2$$

$$+ \frac{\partial^2 w_i}{\partial x^2}\frac{\partial^2 w_i}{\partial s^2} + \frac{1}{R}\frac{\partial^2 w_i}{\partial x^2}\Big] \qquad \text{(II-1)}$$

The total deflection w can be written as

$$W = W_i + W_1 + W_2 \tag{II-2}$$

where w_1 equals the first portion of the additional deflection which follows the form of the initial deviation and w_2 equals the second portion of the additional deflection which has a wave form different from w_i or w_1. Further, let

$$\Gamma = \frac{W_i}{W_i + W_1} = \text{imperfection ratio} \tag{II-3}$$

The compatibility equation can then be rewritten as:

$$\begin{aligned}\nabla^4 F = E\Bigg\{ & \left(\frac{\partial^2 W_2}{\partial x \partial s}\right)^2 - \frac{\partial^2 W_2}{\partial x^2}\frac{\partial^2 W_2}{\partial s^2} - \frac{1}{R}\frac{\partial^2 W_2}{\partial x^2} \\ & + \frac{(1-\Gamma)^2}{\Gamma^2}\left[\left(\frac{\partial^2 W_i}{\partial x \partial s}\right)^2 - \frac{\partial^2 W_i}{\partial x^2}\frac{\partial^2 W_i}{\partial s^2}\right] - \frac{1}{R}\frac{1-\Gamma}{\Gamma}\frac{\partial^2 W_i}{\partial x^2} \\ & + \frac{1}{\Gamma}\left[2\frac{\partial^2 W_2}{\partial x \partial s}\frac{\partial^2 W_i}{\partial x \partial s} - \frac{\partial^2 W_2}{\partial s^2}\frac{\partial^2 W_i}{\partial x^2} - \frac{\partial^2 W_2}{\partial x^2}\frac{\partial^2 W_i}{\partial s^2}\right]\Bigg\}\end{aligned} \tag{II-4}$$

The equilibrium condition in the normal direction derived by the variation of the total potential energy has the following form:

$$D\nabla^4(W-W_i) = \frac{t}{R}\frac{\partial^2 F}{\partial x^2} + t\left(\frac{\partial^2 F}{\partial s^2}\frac{\partial^2 W}{\partial x^2} + \frac{\partial^2 F}{\partial x^2}\frac{\partial^2 W}{\partial s^2}\right.$$

$$\left. - 2\frac{\partial^2 F}{\partial x \partial s}\frac{\partial^2 W}{\partial x \partial s}\right) - P \qquad \text{(II-5)}$$

Deflection Function and Solution. The deflection functions are assumed to be

$$W_i = \Gamma\left[b_2 \cos\frac{mx}{R}\cos\frac{ns}{R} + b_3 \cos\frac{2mx}{R} + b_3 \cos\frac{2ns}{R}\right] \qquad \text{(II-6)}$$

and

$$W_2 = \bar{b}_2 \cos\frac{jx}{R}\cos\frac{ks}{R} + \bar{b}_3 \cos\frac{2jx}{R} + \bar{b}_3 \cos\frac{2ks}{R} \qquad \text{(II-7)}$$

In general, $m \neq j$, and $n \neq k$. From equations (II-3), (II-6), and (II-7), the total deflection has the following form

$$W = b_2\left[\cos\frac{mx}{R}\cos\frac{ns}{R} + (1-\Gamma)\lambda_2 \cos\frac{jx}{R}\cos\frac{ks}{R}\right]$$

$$+ b_3\left[\cos\frac{2mx}{R} + \cos\frac{2ns}{R} + \right.$$

$$(1-\Gamma)\lambda_3\left(\cos\frac{2jx}{R}+\cos\frac{2ks}{R}\right)\Big] \qquad \text{(II-8)}$$

where the magnitudes of Γ, λ_2, and λ_3 are considered to be designated so that only two equations, corresponding to free parameters b_2 and b_3, need be used to find the critical stress. The λ_2 and λ_3 are defined as

$$\lambda_2 = \frac{1}{1-\Gamma}\,\frac{\bar{b}_2}{b_2}$$

$$\lambda_3 = \frac{1}{1-\Gamma}\,\frac{\bar{b}_3}{b_3}$$

The stress function assumes the following form:

$$F = -\frac{\sigma}{2}s^2 + \frac{PR}{2t}x^2 + a_{11}\cos\frac{mx}{R}\cos\frac{ns}{R} + a_{22}\cos\frac{2mx}{R}\cos\frac{2ns}{R}$$

$$+ a_{20}\cos\frac{2mx}{R} + a_{02}\cos\frac{2nx}{R} + c_{11}\cos\frac{jx}{R}\cos\frac{ks}{R} + c_{20}\cos\frac{2jx}{R}$$

$$+ c_{02}\cos\frac{2ks}{R} + c_{22}\cos\frac{2jx}{R}\cos\frac{2ks}{R} + d_1\sin\frac{mx}{R}\sin\frac{jx}{R}\sin\frac{ns}{R}\sin\frac{ks}{R} +$$

$$+ d_2 \cos\frac{2jx}{R}\cos\frac{2ns}{R} + d_3\cos\frac{2mx}{R}\cos\frac{2ks}{R}$$

$$+ d_4 \cos\frac{mx}{R}\cos\frac{jx}{R}\cos\frac{nx}{R}\cos\frac{ks}{R} \tag{II-9}$$

Applying the Galerkin method to both equations (II-4) and (II-5) establishes the following two equations:

$$\frac{\alpha}{1-\Gamma}\left\{\left[1+(1-\Gamma)\frac{\lambda_2^2}{m^2}j^2\right]\bar{\sigma}-\left[\mu+(1-\Gamma)\lambda_2^2\frac{k^2}{m^2}\right]\bar{p}\right\}=f_1 \tag{II-10}$$

$$\frac{\alpha}{1-\Gamma}\left\{\left[1+(1-\Gamma)\lambda_3^2\frac{j^2}{m^2}\right]\bar{\sigma}-\left[\mu+(1-\Gamma)\lambda_3^2\frac{k^2}{m^2}\right]\bar{p}\right\}=f_2 \tag{II-11}$$

where

$$\bar{\sigma}=\sigma R/Et \quad , \quad \bar{p}=pR^2/Et^2 \tag{II-12}$$

In equations (II-10) and (II-11), the f_1 and f_2 are functions of Γ, m, n, j, k, b_2, b_3, R, t, ν, λ_2, and λ_3. The complete expressions for f_1 and f_2 are very long, and will be reduced to specific forms in later discussions.

Depending upon the magnitude of λ_2 and λ_3, there are two limiting cases:

(1) $\lambda_2, \lambda_3 \gg 1$, i.e., most parts of the additional deflection are different from the initial deviation.

(2) $\lambda_2, \lambda_3 \ll 1$, i.e., most parts of the additional deflection follow the same form as the initial deflection.

In order to find which one of the above two cases yields a lower value of the minimum load, an initial study is carried out on the basis of a linear solution. The non-linear solution should change the magnitudes but not reverse the conclusions drawn from the linear analysis.

Linear Solution. For the linear solution, $\lambda_3 = 0$. Equation (II-10) is reduced to the following expression:

$$\frac{\alpha}{1-\Gamma}\left[\left(1+\frac{1-\Gamma}{m^2}\lambda_2^2 j^2\right)\bar{\sigma}-\left(\mu+\frac{1-\Gamma}{m^2}\lambda_2^2 k^2\right)\bar{P}\right]$$

$$=\frac{1}{12(1-\nu^2)}\left[(1+\mu)^2+(k^2+j^2)^2\frac{\lambda_2^2}{m^4}\right]+\alpha^2\left[\frac{1}{(1+\mu)^2}+\frac{j^4\lambda_2^2}{(k^2+j^2)^2}\right] \qquad \text{(II-13)}$$

The symbols α and μ are defined as:

$$\alpha = R/m^2 t$$

$$\mu = n^2/m^2 \qquad \text{(II-14)}$$

After minimization with respect to α ,

$$\bar{\sigma} - \frac{\mu + (1-\Gamma)\lambda_2^2 k^2/m^2}{1 + (1-\Gamma)\lambda_2^2 j^2/m^2}\bar{p} = \frac{1-\Gamma}{\sqrt{3(1-\nu^2)}} \frac{1}{1+(1-\Gamma)\lambda_2^2 j^2/m^2}\left[1 + \frac{(k^2+j^2)^2}{m^4}\frac{\lambda_2^2}{(1+\mu)^2}\right]^{1/2}\left[1 + \frac{(1+\mu)^2}{(k^2+j^2)^2} j^4 \lambda_2^2\right]^{1/2} \tag{II-15}$$

Upon examination of the above equation, the two limiting cases are seen to be:

(1) when $\lambda_2 \gg 1$, $\bar{\sigma} - (k^2/j^2)\bar{p} \approx \dfrac{1}{\sqrt{3(1-\nu^2)}}$ (II-16)

(2) when $\lambda_2 \ll 1$, $\bar{\sigma} \approx \dfrac{1-\Gamma}{\sqrt{3(1-\nu^2)}}$ (II-17)

It can be observed that Case (2) always predicates a lower value of σ . If only the minimum load is of interest, the additional deflection can be thus assumed to retain the same wave-length in both the circumferential and axial directions. Hence, λ_2 and λ_3 are considered to be zero in the finite-deflection analysis made in the following section.

Additional Deflection Following the Wave Form of Initial Deviation

The imperfection ratio, Γ , is proposed as:

$$\Gamma = 1 - \exp(-CR/t) \tag{II-18}$$

The index C is always positive, and is assumed to be a function of internal pressure only. The determination of C will be discussed later. In this part, $w_2 = 0$ (i.e., $\lambda_2 = \lambda_3 = 0$). Equations (II-10) and (II-11) have the following form:

$$\frac{1}{1-\Gamma}\,\phi = \frac{(1+\mu)^2}{12(1-\nu^2)}\frac{1}{\alpha} + \alpha\left\{\frac{1}{(1+\mu)^2} - \left[\frac{4(2+\Gamma)}{(1+\mu)^2} + \frac{1}{2}\right]\mu\eta + \frac{16(1+\Gamma)}{(1+\mu)^2}\mu^2\eta^2\right\} + \frac{(1+\mu^2)(1+\Gamma)}{16\,\alpha}\left(\frac{b_2}{t}\right)^2 \tag{II-19}$$

and

$$\frac{1}{1-\Gamma}\,\phi = \frac{1+\mu^2}{3(1-\nu^2)}\frac{1}{\alpha} + \left[\frac{1}{4} + \frac{4(1+\Gamma)}{(1+\mu)^2}\mu^2\eta^2\right]\alpha + \frac{1}{\alpha}\left\{\frac{2(1+\Gamma)}{(1+\mu)^2}\mu^2 - \frac{\mu}{\eta}\left[\frac{1}{2(1+\mu)^2} + \frac{1+\Gamma}{32}\right]\right\}\left(\frac{b_2}{t}\right)^2 \tag{II-20}$$

In the above equations

$$\phi = \bar{\sigma} - \mu \bar{p} = \frac{\sigma R}{Et} - \mu \frac{pR^2}{Et^2}$$

$$\eta = \frac{b_3}{t} \frac{1}{\alpha} \tag{II-21}$$

After b_2/t is eliminated from equations (II-19) and (II-20), and ϕ is minimized with respect to α, the following expression is obtained:

$$\phi = (1-\Gamma) \sqrt{C_1 C_2} \Big/ \sqrt{3(1-\nu^2)} \tag{II-22}$$

The symbols C_1 and C_2 are defined as follows:

$$\left.\begin{aligned} C_1 &= \frac{A_5 B_1 - A_1 B_5 - A_1 B_6/\eta}{A_1 (A_5 - B_5 - B_6/\eta)} \\ C_2 &= \frac{A_5 B_2 - A_3 B_6 - A_2 B_5 - A_2 B_6/\eta - (A_3 B_5 + A_4 B_6)\eta + (A_5 B_4 - A_4 B_5)\eta^2}{A_2 (A_5 - B_5 - B_6/\eta)} \end{aligned}\right\}$$

(II-23)

where

$$\left.\begin{aligned}
A_1 &= \frac{(1+\mu)^2}{12\,(1-\nu^2)} \\
A_2 &= \frac{1}{(1+\mu)^2} \\
A_3 &= -\left[\frac{4\,(2+\Gamma)}{(1+\mu)^2} + \frac{1}{2}\right]\mu \\
A_4 &= 16\,(1+\Gamma)\,\mu^2/(1+\mu)^2 \\
A_5 &= \frac{1}{16}\,(1+\Gamma)\,(1+\mu^2) \\
B_1 &= (1+\mu^2)/3\,(1-\nu^2) \\
B_2 &= \frac{1}{4} \\
B_4 &= 4\,(1+\Gamma)\,\mu^2/(1+\mu)^2 \\
B_5 &= 2\,(1+\Gamma)\,\mu^2/(1+\mu)^2 \\
B_6 &= -\mu\left[\frac{1}{2\,(1+\mu)^2} + \frac{1+\Gamma}{32}\right]
\end{aligned}\right\} \qquad \text{(II-24)}$$

The next step is to find the minimum ϕ versus η when μ and Γ are given. This minimized value is denoted as $\phi_{\alpha,\eta}$, which is, therefore, a function of μ and Γ. The superscript o is hereafter used to indicate the parameters of perfect shells, for which $\Gamma = 0$ identically. The magnitudes of $\phi^{\circ}_{\alpha,\eta}$ versus μ were found in reference [II-6]

Denote

$$\gamma = \frac{\phi_{\alpha,\eta}}{\phi^{\circ}_{\alpha,\eta}} \tag{II-25}$$

The ratio γ is here called an "imperfection coefficient." The variation of γ with Γ for different values of μ is shown in Fig. II-1. Note that Curve IV ($\mu = 1.15$) is for unpressurized shells, while Curve I ($\mu = 0$) is for shells subject to rather high pressures, for example, $pR^2/Et^2 \geqq 1$. At the same pressure and R/t ratio, Γ remains constant and γ decreases with decreasing μ. From equations (II-21) and (II-25), the minimum compression in the postbuckling region is expressed as

$$\left(\frac{\sigma R}{Et}\right)_{min} = \gamma\, \phi^{\circ}_{\alpha,\eta} + \mu_{cr} \frac{pR^2}{Et^2} \tag{II-26}$$

The notation μ_{cr} represents the value of μ at which the magnitude of $\bar{\sigma}$ is minimum.

The problem, now, is to determine the index C in equation (II-18) . At greater values of the internal pressure p, the wave length ratio μ becomes smaller [II-6] while the imperfection ratio Γ is also expected to be smaller. In Fig. II-1 it can be seen that γ is a decreasing function of Γ but an increasing function of μ. Therefore, the change of pressure should not significantly change the magnitude of γ due to the somewhat counter effect of Γ and μ. For the purpose of evaluating C, it can be assumed that at certain values of R/t:

$$\frac{\bar{\sigma}}{\bar{\sigma}^{\circ}} = \bar{\gamma}$$

In the above equation, $\bar{\gamma}$ is taken as an average value of γ for all pressures. The σ is the actual minimum axial compression found at that R/t ratio. The σ^{o} is the corresponding minimum stress in the perfect shell under the same pressure [II-6] .

After $\bar{\gamma}$ is chosen, the relation between Γ and μ is found from Fig. II-1 . From equation (II-18) , C can be found in terms of Γ and, hence, in terms of μ. Also,

μ can be found in terms of $\bar{p}$ from equation (II-26). The index C is thus determined as a function of $\bar{p}$.

Numerical Evaluation. In this example, $\bar{\gamma}$ is assumed to be 0.6 in one case and 0.52 in another with R/t = 1,500. When $\bar{\gamma}$ is used in Fig. II-1, the variation of Γ with μ is found. The use of equation (II-18) determines C in terms of Γ, and, hence, in terms of μ. When γ is used in equation (II-26), the relation between $\bar{p}$ and μ is obtained when ($\bar{\gamma}\,\phi^{\circ}_{\alpha,\eta}$ + $\mu\,\bar{p}$) is smallest. Note that $\phi^{\circ}_{\alpha,\eta}$ varies with μ [II-6]. The variation of C versus $\bar{p}$ is plotted in Fig. II-2. With this figure and equation (II-18), Γ is determined by $\bar{p}$ and R/t. It should be noted that the γ in equation (II-26) is, in general, a function of Γ and μ (Fig. II-1). When the $\bar{p}$ and R/t are known, Γ is known; thus $\phi^{\circ}_{\alpha,\eta}$ and γ depend on μ only. The $\left(\frac{\sigma R}{Et}\right)_{min}$ is found by assuming different values of μ until the right-hand side of equation (II-26) exhibits its lowest value. The change of $\left(\frac{\sigma R}{Et}\right)_{min}$ with pR^2/Et^2 when R/t = 1,500 is shown in Fig. II-3. The test results from [II-6, II-7, II-8], in which the R/t ratio ranges from greater than 1,000 to less than 1,800, are also adopted in this figure. These test data are much lower than the classical buckling load and are hence considered as the minimum load. The variations of $\left(\frac{\sigma R}{Et}\right)_{min}$, with respect to $\bar{p}$ = 0 and 1, are shown in Fig. II-4. The two curves in this figure serve as upper and lower bounds of minimum loads for imperfect cylinders.

Conclusions

The minimum load was found to be lower when the final buckling pattern had the same wave form as the initial no-load deflection. An imperfection ratio was introduced as an explicit function of R/t and pressure index C. Numerical examples are compared with a group of known experimental results. A similar approach can be used for other types of imperfect shells.

References (II)

1. Donnell, L. H., "A New Theory for the Buckling of Thin Cylinders Under Axial Compression and Bending," Transactions of the ASME, Vol. 56, No. 11, pp. 795-806, November, 1934.

2. Donnell, L. H., and Wan, C. C., "Effect of Imperfections on Buckling of Thin Cylinders and Columns Under Axial Compression," Journal of Applied Mechanics, Vol. 17, No. 1, pp. 73-83, March, 1950.

3. Nash, W. A., "Effect of Large Deflections and Initial Imperfections on the Buckling of Cylindrical Shells Subject to Hydrostatic Pressure," Journal of the Aeronautical Sciences, Vol. 22, No. 4, pp. 264-269, April, 1955.

4. Donnell, L. H., "Effect of Imperfections on Buckling of Thin Cylinders with Fixed Edge Under External Pressure," Proceedings of the Third U.S. National Congress of Applied Mechanics, ASME, pp. 305-311, 1958.

5. Ivanov, V. S., "On the Problem of a Static Elastic Circular Cylindrical Shell with Initial Deflection," Prikladnaia Matematika i Mekhanika (Moscow), Vol. 22, No. 5, pp. 687-690, 1958.

6. Lu, S. Y., and Nash, W. A., "Elastic Instability of Pressurized Cylindrical Shells Under Compression or Bending," Proceedings of the Fourth U.S. National Congress of Applied Mechanics, ASME, pp. 697-704, 1962.

7. Fung, Y. C., and Sechler, E. E., "Buckling of Thin-Walled Circular Cylinders Under Axial Compression and Internal Pressure," Journal of the Aeronautical Sciences, Vol. 24, No. 5, pp. 351-356, May, 1957.

8. Lofblad, R. P., Jr., "Elastic Stability of Thin-Walled Cylinders and Cones with Internal Pressure Under Axial Compression," MIT Technical Report 25-29, May, 1959.

9. Thielemann, W. F., "New Developments in the Nonlinear Theories of the Buckling of Thin Cylindrical Shells," Deutsche Versuchsanstalt fur Luftfahrt E.V. (Mulheim).

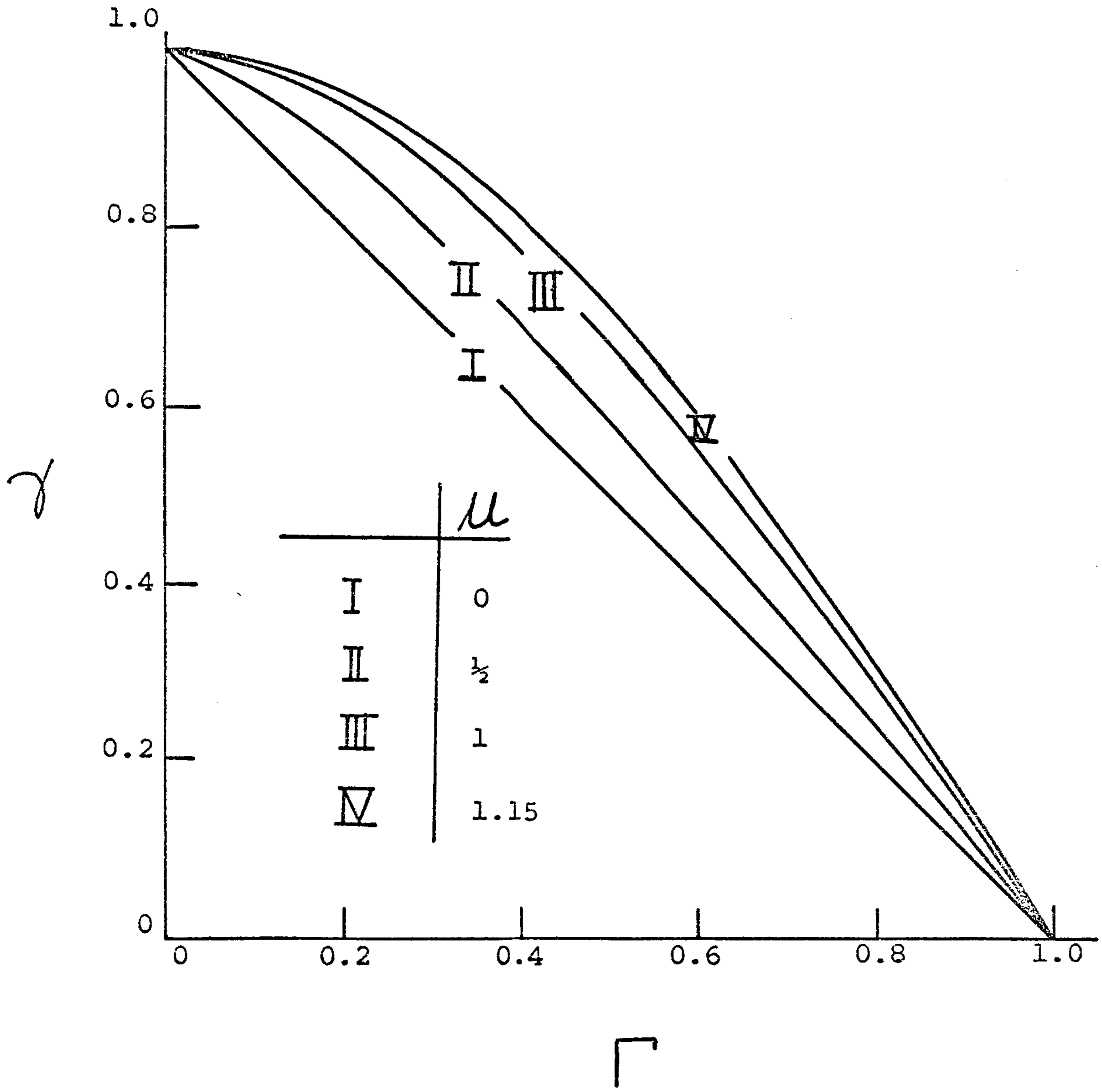

Fig. II-1. Variation of Imperfection Coefficient with Imperfection Ratio

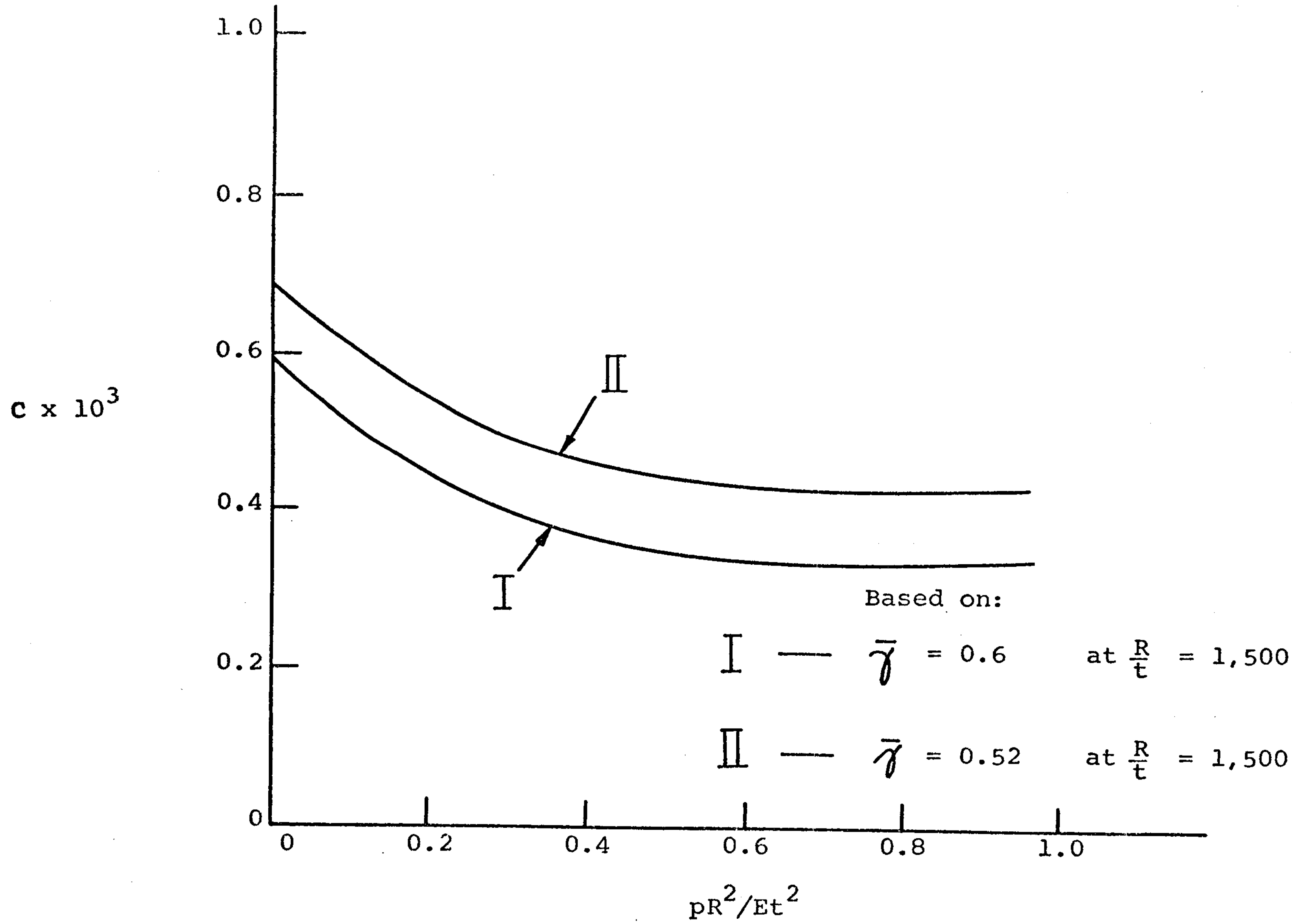

Fig. II-2. Exponential Index C Versus Internal Pressure

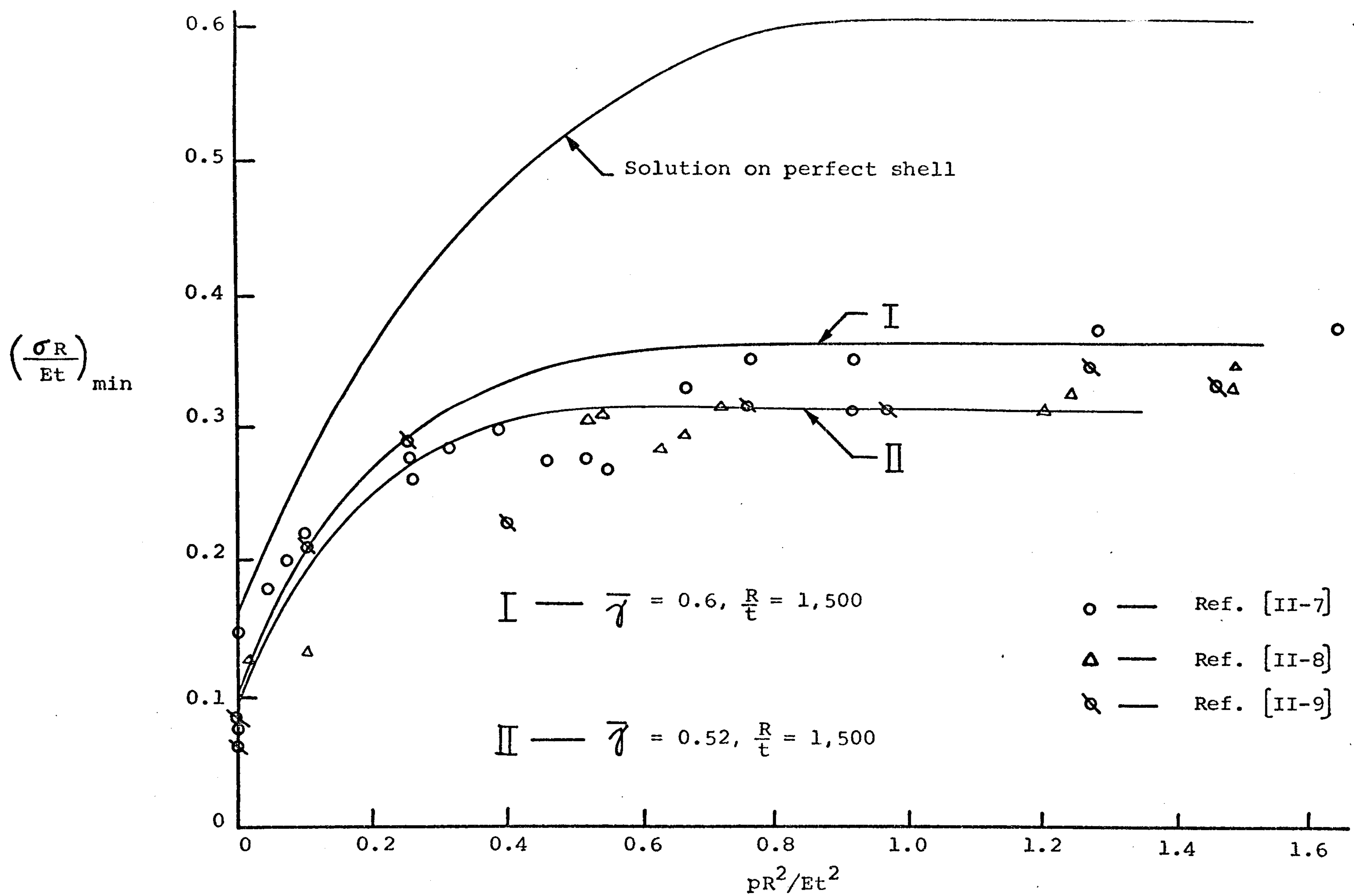

Fig. II-3. Effects of Imperfection

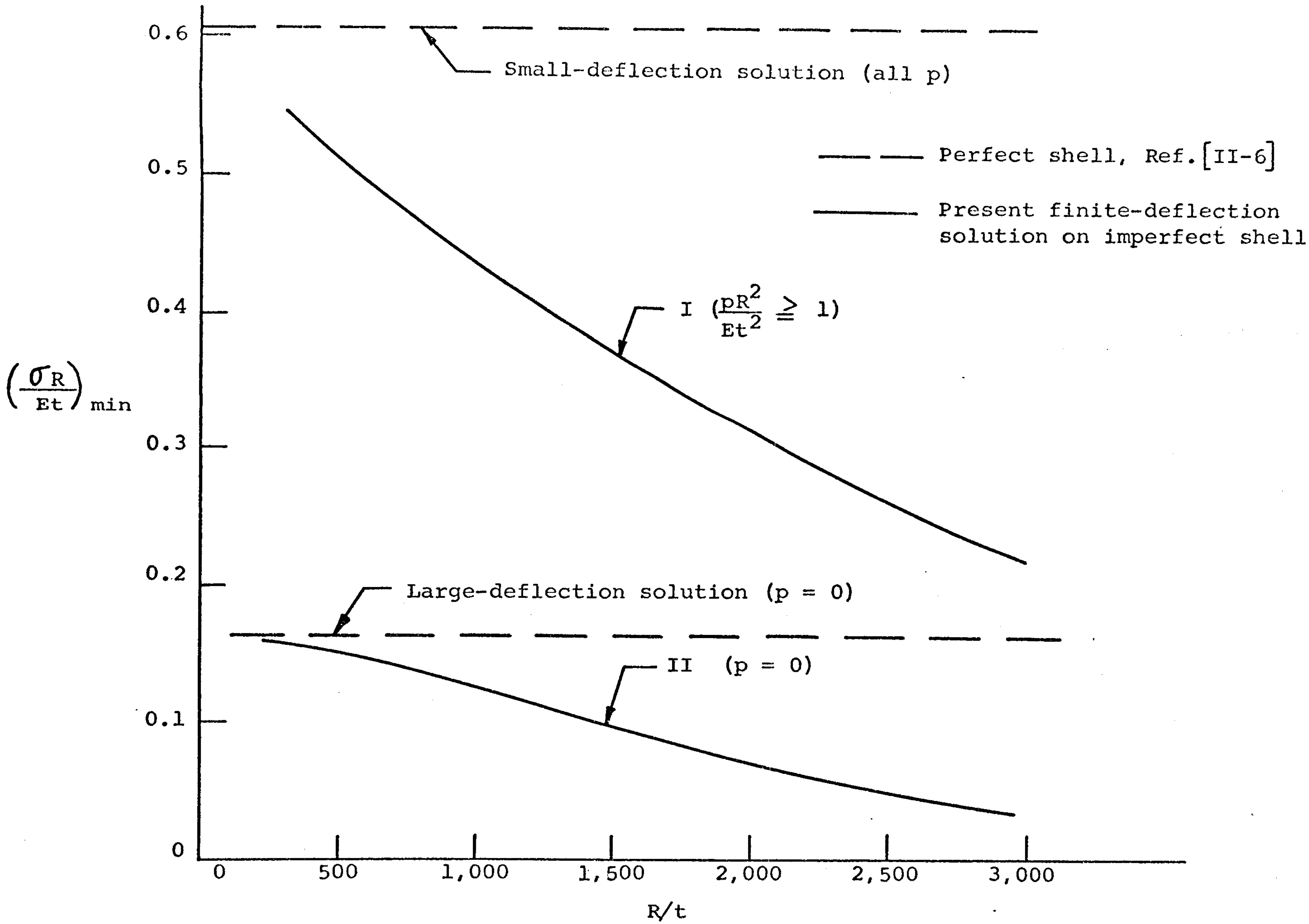

Fig. II-4. Comparison of Solutions

PART III

STABILITY OF STIFFENED PRESSURIZED CYLINDRICAL SHELLS SUBJECT TO COMPRESSION OR BENDING

Introduction

The stability of a stiffened cylindrical shell was recently studied by Becker and Gerard [III-1] by the use of small-deflection, orthotropic-shell theory. In 1958, McCoy [III-2] reported experimental results on the general instability of ring-stiffened, unpressurized, thin cylinders subjected to axial compression. In 1960, Peterson and Dow [III-3] reported test data for a pressurized ring-stiffened cylinder subject to axial compression.

In this part of the present report the general instability of thin pressurized cylinders stiffened by discrete rings is discussed. The cylinders are subject to axial compression or bending. The restoring forces from the stiffeners are introduced in the equilibrium equation by the use of the Dirac delta function. The Galerkin method is used to obtain an approximate solution.

Nomenclature

D	Flexural rigidity
E	Young's modulus

F	Airy stress function
L, R, t	Length, radius and thickness of shell, respectively
N	Number of rings
x, s	Co-ordinates
p	Internal pressure
I	Moment of inertia of stiffeners
J	Twist moment of inertia of stiffeners
δ	Dirac delta
σ	Uniform axial compressive stress
μ	n^2/m^2
∇^2	Laplace operator
∇^4	$(\nabla^2)^2$
i	i-th ring, i = 1, 2, ..., N

Basic Equations

When a shell is reinforced circumferentially by rings, the equilibrium equation can be expressed as

$$D \nabla^4 w + \sum_{i=1}^{N} \left[E_i I_i \frac{\partial^4 w}{\partial s^4} + G_i J_i \frac{\partial^4 w}{\partial x^2 \partial s^2} \right] \cdot \delta(x - x_i)$$

$$= \frac{t}{R} \frac{\partial^2 F}{\partial x^2} + t \left[\frac{\partial^2 F}{\partial x^2} \frac{\partial^2 w}{\partial s^2} - 2 \frac{\partial^2 F}{\partial x \partial s} \frac{\partial^2 w}{\partial x \partial s} + \right.$$

$$+\frac{\partial^2 F}{\partial s^2}\frac{\partial^2 W}{\partial x^2}\Big] - P \qquad \text{(III-1)}$$

In the above equation, $E_i I_i$ and $G_i J_i$ are the bending and torsional rigidities of the i-th ring, respectively. The Dirac delta function is defined as follows:

$$\int_0^L f(x)\,\delta(x - x_i)\,dx = f(x_i) \qquad \text{(III-2)}$$

where

d = space between adjacent rings = $L/(N + 1)$

x_i = id = distance from the origin to the i-th ring (III-3)

The shell is considered isotropic and the compatibility equation is expressed as:

$$\nabla^4 F = E\Big[\Big(\frac{\partial^2 W}{\partial x \partial s}\Big)^2 - \Big(\frac{\partial^2 W}{\partial x^2}\Big)\Big(\frac{\partial^2 W}{\partial s^2}\Big) - \frac{1}{R}\frac{\partial^2 W}{\partial x^2}\Big] \qquad \text{(III-4)}$$

Axisymmetric Compression

For the stiffened cylinder subject to axial compression, the general buckling pattern can be assumed to be

$$W = b_1 + b_2 \cos\frac{mx}{R}\cos\frac{ns}{R} + b_3\cos\frac{2mx}{R} + b_4\cos\frac{2ns}{R} \qquad \text{(III-5)}$$

As an approximation, the Airy stress function F has the following assumed form:

$$F = -\frac{\sigma}{2}s^2 + a_{11}\cos\frac{mx}{R}\cos\frac{ns}{R} + a_{02}\cos\frac{2ns}{R}$$

$$+ a_{20}\cos\frac{2mx}{R} + a_{22}\cos\frac{2mx}{R}\cos\frac{2ns}{R} \qquad \text{(III-6)}$$

After the expressions (III-5) and (III-6) are substituted into equation (III-4) and the Galerkin method is applied, the coefficients of F are found to be:

$$\frac{a_{11}}{Et^2} = \frac{\bar{b}_2}{(1+\mu)^2}\left[\alpha - 2\mu(\bar{b}_3 + \bar{b}_4)\right]$$

$$\frac{a_{22}}{Et^2} = \frac{\mu}{(1+\mu)^2}\bar{b}_3\bar{b}_4$$

$$\frac{a_{02}}{Et^2} = -\frac{\bar{b}_2^2}{32\mu}$$

$$\frac{a_{20}}{Et^2} = \frac{\alpha\bar{b}_3}{4} - \frac{\mu}{32}\bar{b}_2^2 \tag{III-7}$$

where

$$\bar{b}_j = \frac{b_j}{t}$$

$$\mu = \frac{n^2}{m^2}$$

$$\alpha = \frac{R}{m^2 t} \tag{III-8}$$

The integration of (III-1), together with the relations given in (III-8), establishes the following three equations:

$$\bar{\sigma} - \mu \bar{p} = B_2' \frac{\bar{b}_2^2}{\alpha} + \frac{B_4'}{\alpha} + \alpha \left(B_5' + B_6' \eta + B_7' \eta^2 \right) \tag{III-9}$$

$$\bar{\sigma} = \left(C_2' + \frac{C_3'}{\eta} \right) \frac{\bar{b}_2^2}{\alpha} + \frac{C_4'}{\alpha} + \alpha \left(C_5' + C_7' \eta^2 \right) \tag{III-10}$$

$$-\mu \bar{p} = \left(D_2' + \frac{D_3'}{\eta} \right) \frac{\bar{b}_2^2}{\alpha} + \frac{D_4'}{\alpha} + \alpha \left(D_7' \eta^2 \right) \tag{III-11}$$

where

$$\bar{\sigma} = \frac{\sigma R}{E t} \quad , \quad \bar{p} = \frac{p R^2}{E t^2}$$

$$\eta = \frac{\bar{b}_2}{\alpha} \quad , \quad k = \frac{\bar{b}_4}{\bar{b}_3} \tag{III-12}$$

The dimensionless parameters B', C' and D' are used for brevity and defined as:

$$B_2' = \frac{1+\mu^2}{16}$$

$$B_4' = \frac{1}{12(1-\nu^2)}\left[(1+\mu)^2 + \mu^2 \sum_{i=1}^{N} 2\,\bar{I}_i \cos^2\left(\frac{m x_i}{R}\right)\right.$$

$$\left. + \mu \sum_{i=1}^{N} 2\,\bar{J}_i \cos^2\left(\frac{m x_i}{R}\right)\right]$$

$$B_5' = \frac{1}{(1+\mu)^2}$$

$$B_6' = -\mu\left[\frac{1}{2} + \frac{4(1+k)}{(1+\mu)^2}\right]$$

$$B_7' = \frac{4(1+k)^2 \mu^2}{(1+\mu)^2}$$

$$C_2' = \frac{(1+k)\mu^2}{2(1+\mu)^2}$$

$$
\left.
\begin{aligned}
C_3' &= -\frac{\mu}{4}\left[\frac{1}{8} + \frac{1}{(1+\mu)^2}\right] \\[2ex]
C_4' &= \frac{1}{3(1-\nu^2)} \\[2ex]
C_5' &= \frac{1}{4} \\[2ex]
C_7' &= \frac{2k^2\mu^2}{(1+\mu)^2} \\[2ex]
D_2' &= \frac{(1+k)\,\mu^2}{2k(1+\mu)^2} \\[2ex]
D_3' &= \frac{-\mu}{4k(1+\mu)^2} \\[2ex]
D_4' &= \frac{\mu^2\left(1+\sum_{i=1}^{N}\bar{I}_i\right)}{3(1-\nu^2)} \\[2ex]
D_7' &= \frac{2\mu^2}{(1+\mu)^2}
\end{aligned}
\right\}
\qquad \text{(III-13)}
$$

In equations (III-13) ,

$$\bar{I}_i = \frac{E_i I_i}{E\left[\frac{Lt^3}{12(1-\nu^2)}\right]}$$

$$\bar{J}_i = \frac{G_i J_i}{E\left[\frac{Lt^3}{12(1-\nu^2)}\right]} \qquad \text{(III-14)}$$

Axial Bending

When a cylinder is subjected to axial bending, the deflection function is assumed to be

$$W = b_1 + \cos^2\left(\frac{s}{2R}\right)\left[b_2 \cos\frac{mx}{R} \cos\frac{ns}{R} + b_3 \cos\frac{2mx}{R} + b_4 \cos\frac{2ns}{R}\right] \qquad \text{(III-15)}$$

The corresponding Airy stress function F is assumed to be

$$F = a_{11} \cos\frac{mx}{R} \cos\frac{ns}{R} + a_{22} \cos\frac{2mx}{R} \cos\frac{2ns}{R}$$

$$+ a_{20} \cos\frac{2mx}{R} + a_{02} \cos\frac{2ns}{R} - \frac{\sigma_c}{2} S^2$$

$$+ \sigma_b R^2 \cos\frac{s}{R} \qquad \text{(III-16)}$$

where σ_b is the peak bending stress.

Following the same reasoning discussed in Part I, for practical purposes $\frac{1}{m^2}$ and $\frac{1}{m^4}$ are negligible compared to unity in this section. The approach to the present problem is the same as that used for the case of axisymmetric compression. After the equilibrium equation (III-1) is integrated with the use of equations (III-15) and (III-16) , the following three equations are established.

$$\bar{\sigma}_b + \frac{3}{2}\bar{\sigma}_c - \frac{3}{2}\mu\bar{P} = \bar{B}_2' \frac{\bar{b}_2^2}{\alpha} + \frac{\bar{B}_4'}{\alpha}$$

$$+ \alpha\left(\bar{B}_5' + \bar{B}_6'\eta + \bar{B}_7'\eta^2\right) \qquad \text{(III-17)}$$

$$\bar{\sigma}_b + \frac{3}{2}\bar{\sigma}_c = \left(\bar{C}_2' + \frac{\bar{C}_3'}{\eta}\right)\frac{\bar{b}_2^2}{\alpha} + \frac{\bar{C}_4'}{\alpha}$$

$$+ \alpha\left(\bar{C}_5' + \bar{C}_7'\eta^2\right) \tag{III-18}$$

$$-\frac{3}{2}\mu\bar{p} = \left(\bar{D}_2' + \frac{\bar{D}_3'}{\eta}\right)\frac{\bar{b}_2^2}{\alpha} + \frac{\bar{D}_4'}{\alpha}$$

$$+ \alpha\,\bar{D}_7'\,\eta^2 \tag{III-19}$$

where

$$\bar{\sigma}_b = \frac{\sigma_b R}{E t} \quad , \quad \bar{\sigma}_c = \frac{\sigma_c R}{E t} \tag{III-20}$$

In equations (III-17, III-18, III-19), the following symbols are used:

$$\bar{B}_2' = \frac{9(1+\mu^2)}{256}$$

$$\bar{B}_4' = \frac{1}{8(1-\nu^2)}\left[(1+\mu)^2 + \mu^2\sum_{i=1}^{N} 2\,\bar{I}_i \cos^2\left(\frac{m x_i}{R}\right)\right.$$

$$\left. + \mu\sum_{i=1}^{N} 2\,\bar{J}_i \cos^2\left(\frac{m x_i}{R}\right)\right]$$

$$
\left.
\begin{aligned}
\bar{B}_5' &= \frac{1}{(1+\mu)^2} \\[2ex]
\bar{B}_6' &= -\mu \left[\frac{3}{8} + \frac{3(1+k)}{(1+\mu)^2} \right] \\[2ex]
\bar{B}_7' &= \frac{9(1+k)^2 \mu^2}{4(1+\mu)^2} \\[2ex]
\bar{C}_2' &= \frac{9(1+k)\mu^2}{32(1+\mu)^2} \\[2ex]
\bar{C}_3' &= -\frac{3\mu}{16(1+\mu)^2} - \frac{3\mu}{128} \\[2ex]
\bar{C}_4' &= \frac{1}{2(1-\nu^2)} \\[2ex]
\bar{C}_5' &= \frac{1}{4}
\end{aligned}
\right\}
\qquad \text{(III-21)}
$$

$$\bar{C}_7' = \frac{9k^2\mu^2}{8(1+\mu)^2}$$

$$\bar{D}_2' = \frac{(1+k)\,\mu^2}{32k\,(1+\mu)^2}$$

$$\bar{D}_3' = -\frac{3\mu}{16k\,(1+\mu)^2}$$

$$\bar{D}_4' = \frac{\mu^2\left(1+\sum_{i=1}^{N}\bar{I}_i\right)}{2\,(1-\nu^2)}$$

$$\bar{D}_7' = \frac{9\mu^2}{8(1+\mu)^2}$$

Simplified Solution (k = 1)

The solution can be simplified by considering k = 1 (i.e., $b_3 = b_4$). For the case of uniform compression, when k = 1 equations (III-10) and (III-11) are combined into one equation, viz:

$$\bar{\sigma} - \mu \bar{p} = \left(C_2' + D_2' + \frac{C_3' + D_3'}{\eta} \right) \frac{\bar{b}_2^2}{\alpha} + \frac{C_4' + D_4'}{\alpha}$$

$$+ \alpha \left[C_5' + \left(C_7' + D_7' \right) \eta^2 \right] \tag{III-22}$$

When $\bar{b}_2$ is eliminated between (III-9) and (III-22), the following equation is obtained.

$$\bar{\sigma} - \mu \bar{p} = \frac{\Psi_1}{\alpha} + \Psi_2 \alpha \tag{III-23}$$

In the above equation,

$$\Psi_1 = \frac{B_2' \left(C_4' + D_4' \right) - B_4' \left(C_2' + D_2' \right) - B_4' \left(C_3' + D_3' \right) / \eta}{B_2' - \left(C_2' + D_2' \right) - \left(C_3' + D_3' \right) / \eta} \tag{III-24}$$

$$\Psi_2 = \left[B_2' C_5' - B_6' \left(C_3' + D_3' \right) - B_5' \left(C_2' + D_2' \right) \right.$$

$$- B_5' \left(C_3' + D_3' \right) - B_6' \left(C_2' + D_2' \right) \eta - B_7' \left(C_3' + D_3' \right) \eta$$

$$+ B_2'(C_7' + D_7')\eta^2 - B_7'(C_2' + D_2')\eta^2\big]\big[B_2'$$

$$-(C_2' + D_2') - (C_3' + D_3')/\eta\big]^{-1} \tag{III-25}$$

When the shell buckles into multiple waves and the space between two adjacent rings is small compared to the length of the shell, an approximation can be made by assuming

$$\sum_{i=1}^{N} \bar{I}_i \cos^2\left(\frac{m x_i}{R}\right) = \sum_{i=1}^{N} \frac{\bar{I}_i}{2}$$

and

$$\sum_{i=1}^{N} \bar{J}_i \cos^2\left(\frac{m x_i}{R}\right) = \sum_{i=1}^{N} \frac{\bar{J}_i}{2}$$

This assumption implies that the mean values of ring rigidities are used.

From the relation $\frac{\partial \bar{\sigma}}{\partial \alpha} = 0$ and equation (III-23),

$$\bar{\sigma} - \mu \bar{p} = 2\sqrt{\psi_1 \psi_2} \tag{III-26}$$

where Ψ_1 and Ψ_2 are functions of μ and η . The minimum value of $\bar{\sigma}$ can be found for each given value of μ which is equal to the wave length ratio. It is to be noted that $\mu = 1$ may be used for p = 0 and μ decreases when p increases.

Analogous to the solution for the case of axisymmetric compression, the simplified solution for finding the minimum bending stress $\bar{\sigma}_b$ has the following form:

$$\bar{\sigma}_b + \frac{3}{2}\bar{\sigma}_c - \frac{3}{2}\mu\bar{P} = 2\sqrt{\bar{\Psi}_1\bar{\Psi}_2} \tag{III-27}$$

In the above equation,

$$\bar{\Psi}_1 = \frac{\bar{B}_2'(\bar{C}_4' + \bar{D}_4') - \bar{B}_4'(\bar{C}_2' + \bar{D}_2') - \bar{B}_4'(\bar{C}_3' + \bar{D}_3')/\eta}{\bar{B}_2' - (\bar{C}_2' + \bar{D}_2') - (\bar{C}_3' + \bar{D}_3')/\eta} \tag{III-28}$$

$$\bar{\Psi}_2 = [\bar{B}_2'\bar{C}_5' - \bar{B}_6'(\bar{C}_3' + \bar{D}_3') - \bar{B}_5'(\bar{C}_2' + \bar{D}_2')$$

$$- \bar{B}_5'(\bar{C}_3' + \bar{D}_3') - \bar{B}_6'(\bar{C}_2' + \bar{D}_2')\eta$$

$$- \bar{B}_7'(\bar{C}_3' + \bar{D}_3')\eta + \bar{B}_2'(\bar{C}_7' + \bar{D}_7')\eta^2 -$$

$$- \bar{B}_7' \left(\bar{C}_2' + \bar{D}_2' \right) \right] \left[\bar{B}_2' - \left(\bar{C}_2' + \bar{D}_2' \right) \right.$$

$$\left. - \left(\bar{C}_3' + \bar{D}_3' \right) / \eta \right]^{-1} \qquad \text{(III-29)}$$

Conclusions

The effects due to reinforcing rings are included in the parameters B_4' and D_4' [equation (III-13)] for axisymmetric compression and in $\bar{B}_4'$ and $\bar{D}_4'$ [equation (III-21)] for the case of bending. These effects increase with increasing μ. Since μ decreases when the internal pressure p increases, the rings have a greater stiffening effect on the cylindrical shell at lower values of internal pressure. The ratio between the minimum bending stress and the uniform compressive stress is approximately equal to that found for the unstiffened shell in Part II.

References (III)

1. Becker, H., and Gerard, G., "Elastic Stability of Orthotropic Shells," Journal of the Aerospace Sciences, Vol. 29, No. 5, pp. 505-512, May, 1962.

2. McCoy, J. C., "An Experimental Investigation of the General Instability of Ring-Stiffened, Unpressurized, Thin-Walled Cylinders Under Axial Compression," California Institute of Technology, 1958.

3. Peterson, J. P., and Dow, M. B., "Bending and Compression Tests of Pressurized Ring-Stiffened Cylinders," NASA TN D-360, April, 1960.

PART IV

GENERAL INSTABILITY OF RING-STIFFENED CYLINDRICAL SHELLS SUBJECT TO EXTERNAL PRESSURE

Introduction

The buckling under external pressure of a circular cylindrical shell with evenly spaced rings was first investigated by Kendrick in a series of three papers [IV-1]. The general instability of a clamped-end cylindrical shell with stiffening rings was later studied by Nash [IV-2]. An investigation based upon the use of Donnell's linearized equations derived by Taylor for orthotropic cylinders was reported by Becker [IV-3].

In the current study a finite-deflection analysis is made of the buckling of cylindrical shells stiffened with rings and subjected to external pressure. The method of minimum potential energy is employed. The ends of the cylinders are taken to be simply supported, and the deflection configuration involves five free parameters. This leads to a system of five nonlinear algebraic equations in five unknowns.

Nomenclature

E	Young's modulus
R, t, L	Radius, thickness, and length of shell, respectively
N	Number of rings

H	$N + 1$
A_i	Sectional area of i-th ring
I_i	Moment of inertia of i-th ring
n	Number of circumferential waves
u, v, w	Displacements in axial, circumferential and radial directions, respectively
q	External pressure
h_r	t/R
h_ℓ	t/L
α_i	$E_i A_i (1 - \nu^2)/EtL$
β_i	$E_i I_i (1 - \nu^2)/EtLR^2$

Potential Energy

The approximate strain-displacement relations of finite-deflection theory can be expressed as:

$$\left.\begin{aligned} \epsilon_x &= \frac{\partial u}{\partial x} + \frac{1}{2}\left(\frac{\partial w}{\partial x}\right)^2 \\ \epsilon_s &= \frac{\partial v}{\partial s} + \frac{1}{2}\left(\frac{\partial w}{\partial s}\right)^2 - \frac{w}{R} \\ \epsilon_{xs} &= \frac{\partial v}{\partial x} + \frac{\partial u}{\partial s} + \frac{1}{2}\frac{\partial w}{\partial x}\frac{\partial w}{\partial s} \end{aligned}\right\} \qquad \text{(IV-1)}$$

The extensional strain energy of the shell is

$$\mathcal{U}_e = \frac{Et}{2(1-\nu^2)} \int_0^L \int_0^{2\pi R} \Big[\epsilon_x^2 + \epsilon_s^2 + 2\nu\, \epsilon_x \epsilon_s + \frac{1-\nu}{2} \epsilon_{xs}^2 \Big] \, dx \, ds \tag{IV-2}$$

The bending strain energy of the shell is

$$\mathcal{U}_b = \frac{Et^3}{24(1-\nu^2)} \int_0^L \int_0^{2\pi R} \Big[\left(\frac{\partial^2 w}{\partial x^2}\right)^2 + 2\nu \frac{\partial^2 w}{\partial x^2} \frac{\partial^2 w}{\partial s^2} + \left(\frac{\partial^2 w}{\partial s^2}\right)^2 + 2(1-\nu)\left(\frac{\partial^2 w}{\partial x \partial s}\right)^2 \Big] \, dx \, ds \tag{IV-3}$$

The extensional strain energy of the i-th ring is

$$\mathcal{U}_{e,i} = \frac{E_i A_i}{2} \int_0^{2\pi R} (\epsilon_s)^2_{x=x_i} \, ds \tag{IV-4}$$

where x_i is the distance from one end, $(x = 0)$, to the i-th ring. The bending energy of the i-th ring is

$$\mathcal{U}_{b,i} = \frac{E_i I_i}{2} \int_0^{2\pi R} \left[\left(\frac{\partial^2 w}{\partial s^2} \right)^2 + 2 \frac{w}{R^2} \frac{\partial^2 w}{\partial s^2} + \frac{w^2}{R^4} \right]_{x = x_i} ds \qquad \text{(IV-5)}$$

The potential of the radial pressure is

$$\bar{W} = q \left\{ \bar{\epsilon} L \pi R^2 + R \int_0^L \int_0^{2\pi R} \left[\frac{w}{R} - \frac{v^2}{2R^2} \right.\right.$$

$$\left.\left. - \frac{v^2}{2R^2} - \frac{w^2}{2R^2} - \frac{u}{R} \frac{\partial w}{\partial x} - \frac{v}{R} \frac{\partial w}{\partial s} \right] dx\, ds \right\} \qquad \text{(IV-6)}$$

The total potential energy is

$$U = U_e + U_b + \sum_{i=1}^{N} U_{e,i} + \sum_{i=1}^{N} \mathcal{U}_{b,i} - \bar{W} \qquad \text{(IV-7)}$$

Displacement Functions

For simply supported cylinders, the displacement functions have the following assumed forms:

$$
\begin{aligned}
w &= t\left(d_1 \sin\frac{\pi x}{L} \cos\frac{ns}{R} + d_2 \sin^2\frac{\pi x}{L_f} \cos\frac{ns}{R} \right) \\
u &= t\, d_3 \cos\frac{\pi x}{L} \cos\frac{ns}{R} \qquad \text{(IV-8)} \\
v &= t\left[d_4 \sin\frac{\pi x}{L} + d_5 \sin^2\left(\frac{\pi x}{L_f}\right) \right] \sin\frac{ns}{R}
\end{aligned}
$$

where $L_f = \dfrac{L}{N + 1}$ = average spacing between two rings. The nondimensional parameters d_1, d_2, d_3, d_4 and d_5 are arbitrary.

Collapse Pressure

For the condition of equilibrium, the variation of the total potential U [equation (IV-7)] with respect to each of the parameters d_1, d_2, d_3, d_4, and d_5 must be zero. This leads to the following relations:

$$
\frac{\partial U}{\partial d_1} = \frac{\partial U}{\partial d_2} = \frac{\partial U}{\partial d_3} = \frac{\partial U}{\partial d_4} = \frac{\partial U}{\partial d_5} = 0 \qquad \text{(IV-9)}
$$

The above equations lead to a series of five nonlinear algebraic equations which are written in the brief forms:

$$\frac{M_1}{K_1} = \frac{M_2}{K_2} = \frac{M_3}{K_3} = \frac{M_4}{K_4} = \frac{M_5}{K_5} = -\frac{\rho R}{Et}\left(1-\nu^2\right) \tag{IV-10}$$

In equation (IV-10), the M and K represent the following expressions.

$$M_1 = \lambda_1 d_1 + \lambda_2 d_1^3 + \lambda_3 d_2 + \lambda_4 d_1^2 d_2 + \lambda_5 d_2^2 d_1 + \lambda_6 d_2^3 + \lambda_7 d_3 + \lambda_8 d_4 + \lambda_9 d_5 \quad , \tag{IV-11}$$

$$K_1 = e_1 d_1 + e_2 d_3 + e_3 d_1 + e_4 d_4 + e_5 d_5 \quad , \tag{IV-12}$$

$$M_2 = \lambda_3 d_1 + \frac{1}{3}\lambda_4 d_1^3 + \lambda_{10} d_2 + \lambda_5 d_1^2 d_2 + 3\lambda_6 d_1 d_2^2 + \lambda_{11} d_2^3 + \lambda_{12} d_3 + \lambda_{13} d_4 + \lambda_{14} d_5 \quad , \tag{IV-13}$$

$$K_2 = e_1 d_1 + \frac{3}{4} e_3 d_2 + e_6 d_3 + e_7 d_4$$

$$+ e_8 d_5 \quad , \tag{IV-14}$$

$$M_3 = \lambda_7 d_1 + \lambda_{15} d_2 + \lambda_{16} d_3 + \lambda_{17} d_4$$

$$+ \lambda_{18} d_5 \quad , \tag{IV-15}$$

$$K_3 = e_2 d_1 + e_6 d_2 \quad , \tag{IV-16}$$

$$M_4 = \lambda_{17} d_3 + \lambda_8 d_1 + \lambda_{19} d_4 + \lambda_{20} d_5$$

$$+ \lambda_{13} d_2 \quad , \tag{IV-17}$$

$$K_4 = e_4 d_1 + e_3 d_4 + e_9 d_5 + e_7 d_2 \quad , \tag{IV-18}$$

$$M_5 = \lambda_{18} d_3 + \lambda_9 d_1 + \lambda_{20} d_4 + \lambda_{21} d_5$$

$$+ \lambda_{14} d_2 \quad , \qquad \text{(IV-19)}$$

$$K_5 = e_5 d_1 + e_9 d_4 + e_{10} d_5 + e_8 d_2 \quad , \qquad \text{(IV-20)}$$

The symbols λ_j and e_j used in equations (IV-11) to (IV-20) have the relations defined below.

$$\lambda_1 = \pi \frac{h_r}{h_e} + \frac{\pi}{12} h_r h_e \left[\pi^2 \frac{h_e}{h_r} + n^2 \frac{h_r}{h_e} \right]^2$$

$$+ 2\pi \frac{h_r}{h_e} \sum_{i=1}^{N} \left[(1 - n^2)^2 \beta_i + \alpha_i \right] \sin^2\left(\frac{\pi x_i}{L} \right) \quad ,$$

$$\lambda_2 = \frac{\pi}{32} h_r h_\ell \left[9\pi^4 \frac{h_\ell^2}{h_r^2} + 9n^4 \frac{h_r^2}{h_\ell^2} + 2n^2\pi^2 \right.$$

$$\left. + 24n^4 \frac{h_r^2}{h_\ell^2} \sum_{i=1}^{N} \alpha_i \sin^4\left(\frac{\pi x_i}{L}\right)\right] ,$$

$$\lambda_3 = \left(1 + \frac{1}{4H^2-1}\right)\left(\frac{h_r}{h_\ell}\right)\left[2 + \frac{n^4}{6} h_r^2 \right.$$

$$\left. + \frac{\nu}{6} n^2 \pi^2 h_\ell^2 \right] + \left(\frac{2}{4H^2-1}\right)\left(\frac{H^2\pi^2}{3} h_r h_\ell\right)$$

$$\left(\nu n^2 + \pi^2 \frac{h_\ell^2}{h_r^2}\right) + \left(\frac{4H^2}{4H^2-1}\right)\left(\frac{1-\nu}{3}\right)\left(\frac{1-\nu}{3}\right)\left(n^2\pi^2 h_r h_\ell\right),$$

$$\lambda_4 = \frac{3}{4} h_r h_\ell \left[3H^2\pi^4 \left(\frac{h_\ell^2}{h_r^2}\right)\left(\frac{1}{4H^2-9} + \frac{3}{4H^2-1}\right) \right.$$

$$+ \frac{3}{4} n^4 \frac{h_r^2}{h_\ell^2}\left(\frac{8}{3} + \frac{3}{4H^2-1} - \frac{3}{4H^2-9}\right) + n^2\pi^2 (H_1^2)$$

$$\left. \left(\frac{1}{4H^2-1} - \frac{1}{4H^2-9}\right) + n^2\pi^2 \left(\frac{1}{4}\right)\left(\frac{4}{3} + \frac{1}{4H^2-1} + \frac{3}{4H^2-9}\right) \right] ,$$

$$\lambda_5 = h_r h_\ell \Big[\frac{9}{16} H^2 \pi^5 \frac{h_\ell^2}{h_r^2} + \frac{27}{64} \pi n^4 \frac{h_r^2}{h_\ell^2}$$

$$+ \frac{n^2 \pi^3}{64} \left(3 + \frac{13}{2} H^2 \right) \Big] \quad ,$$

$$\lambda_6 = h_r h_\ell \Big[\frac{9}{4} \pi^4 \frac{h_\ell^2}{h_r^2} H^4 \left(\frac{1}{4H^2-1} - \frac{1}{36H^2-1} \right)$$

$$+ \frac{3}{64} n^4 \frac{h_r^2}{h_\ell^2} \left(\frac{1}{36H^2-1} - \frac{6}{16H^2-1} + \frac{15}{4H^2-1} + 10 \right)$$

$$+ \frac{H^2 n^2 \pi^2}{16} \left(2 + \frac{1}{4H^2-1} + \frac{2}{16H^2-1} - \frac{1}{36H^2-1} \right)$$

$$+ \frac{H^2 n^2 \pi^2}{16} \left(\frac{5}{4H^2-1} - \frac{8}{16H^2-1} + \frac{3}{36H^2-1} \right) \Big] ,$$

$$\lambda_7 = \pi^2 \nu$$

$$\lambda_8 = -n\pi \frac{h_r}{h_\ell} \Big[1 + 2 \sum_{i=1}^{N} \alpha_i \sin^2 \left(\frac{\pi x_i}{L} \right) \Big] ,$$

$$\lambda_9 = -2n\frac{h_r}{h_\ell}\left(1+\frac{1}{4H^2-1}\right)$$

$$\lambda_{10} = \pi\left[\frac{3}{4}\frac{h_r}{h_\ell} + \frac{1}{3}H^4\pi^4\frac{h_\ell^3}{h_r} + \frac{1}{16}n^4\frac{h_r^3}{h_\ell}\right.$$

$$\left. + \frac{1}{6}n^2\pi^2H^2 h_r h_\ell\right] ,$$

$$\lambda_{11} = \frac{9}{32}H^4\pi^5\frac{h_\ell^3}{h_r} + n^4\frac{h_r^3}{h_\ell}\left(\frac{105}{512}\pi\right) ,$$

$$\lambda_{12} = 2\nu\pi\left(1+\frac{1}{4H^2-1}\right) ,$$

$$\lambda_{13} = -\frac{2nh_r}{h_\ell}\left(1+\frac{1}{4H^2-1}\right) ,$$

$$\lambda_{14} = -\frac{3}{4}\frac{h_r}{h_\ell}n\pi ,$$

$$\lambda_{15} = 2\pi\nu\left(1+\frac{1}{4H^2-1}\right) ,$$

$$\lambda_{16} = \pi^3 \frac{h_\ell}{h_r} + \frac{1-\nu}{2} \frac{h_r}{h_\ell} n^2 \pi \quad ,$$

$$\lambda_{17} = -\frac{1+\nu}{2} n \pi^2 \quad ,$$

$$\lambda_{18} = -(1-\nu)\, n \pi H^2 \left(\frac{4}{4H^2-1} \right)$$

$$-2\nu n \pi \left(1 + \frac{1}{4H^2-1} \right) ,$$

$$\lambda_{19} = \frac{1-\nu}{2} \frac{h_\ell}{h_r} \pi^3 + n^2 \pi \frac{h_r}{h_\ell} \Big[1 +$$

$$2 \sum_{i=1}^{N} \alpha_i \sin^2 \left(\frac{\pi X_i}{L} \right) \Big] \quad ,$$

$$\lambda_{20} = (1-\nu)\, \pi^2 H^2 \frac{h_\ell}{h_r} \left(\frac{4}{4H^2-1} \right)$$

$$+ 2 n^2 \frac{h_r}{h_\ell} \left(1 + \frac{1}{4H^2-1} \right) \quad ,$$

$$\lambda_{21} = \frac{1-\nu}{2}\pi^3 H^2 \frac{h_\ell}{h_r} + \frac{3}{4}\frac{h_r}{h_\ell} n^2 \pi \quad , \qquad \text{(IV-21)}$$

$$e_1 = \frac{2h_r}{h_\ell}\left(1+\frac{1}{4H^2-1}\right),$$

$$e_2 = \pi^2 \quad ,$$

$$e_3 = \pi \frac{h_r}{h_\ell} \quad ,$$

$$e_4 = -\pi n \frac{h_r}{h_\ell} \quad ,$$

$$e_5 = -2n\frac{h_r}{h_\ell}\left(1+\frac{1}{4H^2-1}\right) \quad ,$$

$$e_6 = \pi\left(\frac{8H^2}{4H^2-1}\right) \quad ,$$

$$e_7 = -2n\frac{h_r}{h_\ell}\left(1+\frac{1}{4H^2-1}\right) \quad ,$$

$$e_8 = -\frac{3}{4}\frac{h_r}{h_\ell} n\pi \quad ,$$

$$e_9 = 2(1-\nu^2)\frac{h_r}{h_\ell}\left(1+\frac{1}{4H^2-1}\right) \quad ,$$

$$e_{10} = \frac{3}{4}\frac{h_r}{h_\ell}\pi \quad . \qquad \text{(IV-22)}$$

With the given data of the shell and rings and the assumed value of n, the λ_j and e_j in equations (IV-21) and (IV-22) are calculated. These values are substituted into equations (IV-11) to (IV-20). Then the collapse pressure q can be determined by solving the five equations in equations (IV-10) simultaneously.

References (IV)

1. Kendrick, S., "The Buckling Under External Pressure of Circular Cylindrical Shells with Evenly Spaced Equal Strength Circular Ring Frames. Parts I, II, III," Naval Construction Research Establishment (Dunfermline, Scotland), Report N.C.R.E./R211, R243, R244, 1953.

2. Nash, William A., "General Instability of Ring-Reinforced Cylindrical Shells Subject to Hydrostatic Pressure," Proceedings of the Second U.S. National Congress of Applied Mechanics, ASME, pp. 359-368, 1954.

3. Becker, H., "General Instability of Stiffened Cylinders," NACA TN 4237, 1958.

PART V

EFFECT OF SURFACE SHEAR ON BUCKLING OF CYLINDRICAL SHELLS

In this part, a thin-walled circular cylindrical shell is assumed to be under surface shear loading in the longitudinal direction (Fig. V-1). When the surface shear τ varies with x only, the additional compression at one end of the cylinder is

$$P_1 \doteq 2\pi R \int_0^{\ell} \tau(x)\, dx$$

By the principle of superposition, the shear τ can be considered as a combination of two parts. From Fig. V-2,

$$\tau = \tau_1 + \tau_2 \tag{V-1}$$

In the present case

$$\tau_1 = \tau_2 = \frac{\tau}{2} \tag{V-2}$$

The role of τ_1 can be considered that of a body force component in the x direction. Hence, the equilibrium conditions in the x and y directions are, respectively,

$$\frac{\partial \sigma_x}{\partial x} + \frac{\partial \sigma_{xy}}{\partial y} + \frac{2\tau_1}{t} = 0$$

$$\frac{\partial \sigma_y}{\partial y} + \frac{\partial \sigma_{xy}}{\partial x} = 0 \qquad \text{(V-3)}$$

The potential function V is introduced such that

$$\frac{\partial V}{\partial x} = -\frac{\tau}{t} \quad , \quad \frac{\partial V}{\partial y} = 0 \qquad \text{(V-4)}$$

When equations (V-4) are substituted in equations (V-3) and the terms due to large deflection in the radial direction are included, the compatibility equation has the following form:

$$\nabla^2(\sigma_x + \sigma_y) = (1+\nu)\,\nabla^2 V + f(w) \qquad \text{(V-5)}$$

In the above equation

$$f(w) = E\left[\left(\frac{\partial^2 W}{\partial x \partial y}\right)^2 - \left(\frac{\partial^2 W}{\partial x^2} \frac{\partial^2 W}{\partial y^2}\right) - \frac{1}{R} \frac{\partial^2 W}{\partial x^2} \right] \tag{V-6}$$

where ν is Poisson's ratio, w the radial deflection, and ∇^2 the Laplacian operator.

The stress functions $\varphi(x, y)$ are defined by

$$\sigma_x - V = \frac{\partial^2 \varphi}{\partial y^2} \quad , \quad \sigma_y - V = \frac{\partial^2 \varphi}{\partial x^2}$$

$$\sigma_{xy} = -\frac{\partial^2 \varphi}{\partial x \partial y} \tag{V-7}$$

From equations (V-7) and (V-5), the compatibility equation becomes

$$\nabla^4 \varphi = -(1-\nu)\nabla^2 V + E\left[\left(\frac{\partial^2 W}{\partial x \partial y}\right)^2 - \left(\frac{\partial^2 W}{\partial x^2}\right)\left(\frac{\partial^2 W}{\partial y^2}\right) - \frac{1}{R} \frac{\partial^2 W}{\partial x^2} \right] \tag{V-8}$$

The equilibrium condition in the radial direction and the equilibrium relations of moments are found by modifying those given in [V-1] . These relations are:

$$\frac{\partial Q_x}{\partial x} + \frac{\partial Q_y}{\partial y} + t\left[\sigma_y\left(\frac{1}{R} + \frac{\partial^2 w}{\partial y^2}\right) + \sigma_x \frac{\partial^2 w}{\partial x^2} + 2\sigma_{xy}\frac{\partial^2 w}{\partial x \partial y}\right]$$

$$+ 2\tau_1 \frac{\partial w}{\partial x} = 0 \qquad \text{(V-9)}$$

$$\frac{\partial M_x}{\partial x} - \frac{\partial M_{xy}}{\partial y} - Q_x - \tau_2 t = 0 \qquad \text{(V-10)}$$

$$\frac{\partial M_y}{\partial y} - \frac{\partial M_{xy}}{\partial x} - Q_y = 0 \qquad \text{(V-11)}$$

From equations (V-9), (V-10), and (V-11), the equilibrium equation can be expressed as:

$$D\nabla^4 w = t\left[\sigma_y\left(\frac{1}{R} + \frac{\partial^2 w}{\partial y^2}\right) + \sigma_x \frac{\partial^2 w}{\partial x^2} + 2\sigma_{xy}\frac{\partial^2 w}{\partial x \partial y}\right]$$

$$+ \frac{t^2}{2}\nabla^2 V - t\frac{\partial V}{\partial x}\frac{\partial w}{\partial x} \qquad \text{(V-12)}$$

The solution can be found from coupling equation (V-8) with equation (V-12). It should be noted that these equations are analogous to the thermoelastic problems of thin cylindrical shells. When the shear τ is constant, when the effect due to τ_2 [see equation (V-10)] is neglected, and when the radial deflection is small, the problem becomes the one solved in [V-2].

References (V)

1. Timoshenko, S., and Gere, J. M., "Theory of Elastic Stability," 2nd ed., McGraw-Hill Book Co., Inc., pp. 448-453, 1961.

2. Weingarten, V. I., "The Buckling of Cylindrical Shells Under Longitudinally Varying Loads," Journal of Applied Mechanics, Vol. 29, pp. 81-85, 1962.

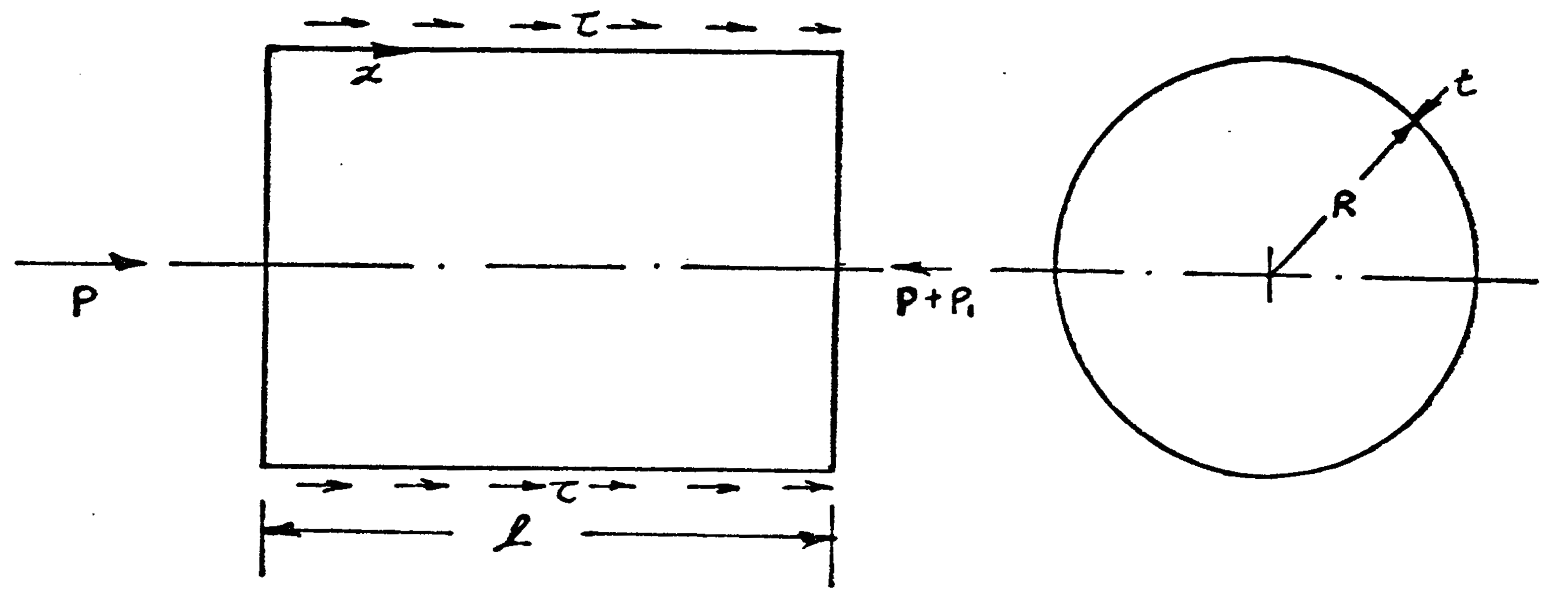

Fig. V-1. Cylinder Under Longitudinal Shear and Axial Compression

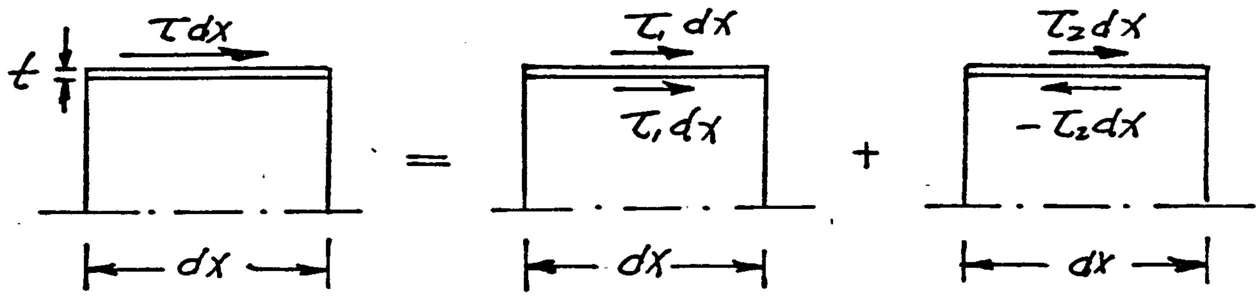

Fig. V-2. Equivalence of Shear Forces (t = Wall-Thickness)